The Paleoenvironmental and Astrobiological Significance of Tufas in the Santa Cruz Region

A Thesis submitted to the faculty of

San Francisco State University

In partial fulfillment of

the requirements for

the Degree

Master of Science

In

Geoscience

by

Maura Colleen Kanner

San Francisco, California

May 2021

Certification of Approval

I certify that I have read The Paleoenvironmental and Astrobiological Significance of Tufas in the Santa Cruz Region by Maura Colleen Kanner, and that in my opinion this work meets the criteria for approving a thesis submitted in partial fulfillment of the requirement for the degree Master of Science in Geoscience at San Francisco State University.

Yadira Ibarra, Ph.D.
Assistant Professor,
Thesis Committee Chair

Erin Bray, Ph.D.
Assistant Professor

Petra Dekens, Ph.D.
Associate Professor

The Paleoenvironmental and Astrobiological Significance of Tufas in the Santa Cruz Region

Maura Colleen Kanner
San Francisco, California
2021

Tufas—carbonates that form in ambient-temperature, freshwater settings—are valuable paleoenvironmental proxies of their depositional conditions. In this study, we use tufa deposits from the Santa Cruz, CA region to (i) model regional paleohydroclimate and (ii) investigate controls of biosignature formation at multiple spatial scales. Previously undescribed inactive, spring-associated tufa mounds (~2 m wide and each over 1 m thick) from Henry Cowell State Park and Pogonip Park were investigated in this study. Henry Cowell additionally hosts carpeted, fluvial tufa adjacent to an active tufa-depositing spring. Infrared stimulated luminescence (IRSL) dating was used on cores collected from the two inactive mounds to determine the timing of carbonate growth. Radiocarbon (^{14}C) dating was carried out on charcoal fragments from the fluvial carbonates at Henry Cowell State Park. IRSL and ^{14}C dates of samples collected from the two sites agree with the age models from other proxies of past pluvial periods in the region (~16 to 5 ka). A piece of charcoal revealed the fluvial carbonates are relatively younger in age (853 ± .04 years BP) and likely represent recent or modern flow conditions. Decimeter-scale samples collected from Henry Cowell State Park were used for petrographic analysis and biosignature investigation. Microscopic investigations using light microscopy revealed specific biological and mineralogical controls on the meso (cm-scale) to macroscopic (m-scale) morphologies. Distinct light and dark calcite bands (~0.1-0.5 mm in thickness) were identified in all samples collected from Henry Cowell State Park suggesting seasonal growth patterns. The presence of the calcite microstructure of *Oocardium stratum*, a freshwater algae that is endemic to tufa environments at both sites, implies the inactive mounds formed under high stream velocities and are of meteoric

origin. In the fluvial carbonates, decimeter-scale tufa mounds grow concentrically and vertically and display smaller domes (several cm in diameter), most of which contain smaller protuberances (several mm in diameter)—a cauliflower-like fabric. The mm-scale protuberances are internally laminated making them a clear astrobiological target due to their stromatolitic morphology. Diatoms were also found in the crust of samples collected from both perched and fluvial carbonates, further indicating biotic influence on tufa formation at the mm- to micro scales. As the first multiscale and chronological analysis of tufas in the Santa Cruz region, this work lays the groundwork for future analyses that will further corroborate their paleoenvironmental and astrobiological significance.

Preface and/or Acknowledgements

I would like to thank my incredible advisor Dr. Yadira Ibarra for all her guidance, unfaltering support, and for going above and beyond to help make me the scientist I am today. I would also like to thank Dr. Erin Bray and Dr. Petra Dekens for serving on my thesis committee. I am deeply grateful for Dave Dempsey and his family, whose generosity via the Dempsey Fellowship gave me the financial means to attend graduate school. I thank the California State Park's Santa Cruz District and the City of Santa Cruz Parks Division for access to the research site. Big thanks to Sebastian Huot for carrying out the IRSL analyses used in this study. Thank you to my parents and my partner Shintaro Noguchi for their enthusiasm and unwavering support. Lastly, I would like to thank my network of friends who cheered me on along the way. Specifically, Megan Mortimer-Lamb and Hannah Schubloom whose mentorship and influence guided me to and through my higher education.

I would like to dedicate this work to my late-grandmother, Irma Kanner, who taught me the importance of selflessness, education, and, above all, happiness.

This work was done on the land of the Awaswas-speaking people of the Ohlone tribe in Santa Cruz, CA (Aulinta).

Table of Contents

List of Tables

List of Figures

List of Appendices

1. Introduction

Tufas are terrestrial carbonates that form from ambient temperature spring water (Ford and Pedley, 1996) and can serve as potential archives of paleoclimate (Andrews, 2006) as well as proxies for biosignatures of ancient life (Potter-McIntyre et al., 2017). The carbonates trap and entomb the aquatic microbial life that thrives in these freshwater settings. The calcification of microorganisms (predominantly algae) and tufa growth is influenced by environmental conditions (Andrews & Brasier, 2005; Andrews, 2006; Merz-Preiß and Riding, 1999; Matsuoka et al., 2001; Sancho et al., 2015; Kano et al., 2003; Capezzuoli et al., 2014) that can fluctuate seasonally to form mm-scale layers (Andrews, 2006; Andrews and Brasier, 2005; Arenas et al., 2014; Ford and Pedley, 1996; Kano et al., 2003; Matsuoka et al., 2001). Environmental factors that affect the morphologies and seasonal deposition of tufa include water temperature, stream velocity, water chemistry, water depth, distance from the spring input, and the physiological activity of flora and bacteria (Arenas et al., 2014; Andrews and Brasier, 2005; Capezzuoli et al., 2014). Analyzing tufa morphologies at different scales can reveal depositional information about (1) hydroclimate and (2) aquatic microbial communities. Given their rapid rates of formation, tufas present the opportunity to study seasonality as well as relatively short-lived climatic events (Andrews, 2006; Arenas & Jones, 2017).

1.1 Aims of Research

This study investigates previously undescribed tufa deposits from two sites in the Santa Cruz, CA region: Pogonip Park and Henry Cowell State Park (Fig. 1). Ancient (>1,000 years) samples were collected from each site and modern samples (<1,000 years) were collected from

Henry Cowell State Park. Ancient tufa was used to assess paleohydroclimate conditions during tufa deposition via petrographic analysis, Infrared Stimulated Luminescence Dating (IRSL) and radiocarbon dating. Examples of modern and ancient tufa were used to establish biosignature preservation at multiple scales (Fig. 4). The aims of these analyses are to (i) constrain the timing of deposition of the ancient tufa mounds; (ii) describe the environment in which the tufa formed; (iii) establish distinguishable biosignatures at multiple scales that can be detected by current rover technology on other planets. Results from this research will help inform models of future and past changes in hydroclimate in a region projected to experience continued drying under the influence of anthropogenic climate change (Cook et al., 2010) and will help guide future astrobiological studies on other rocky planets.

Figure 1. Geologic Map of Santa Cruz County, CA

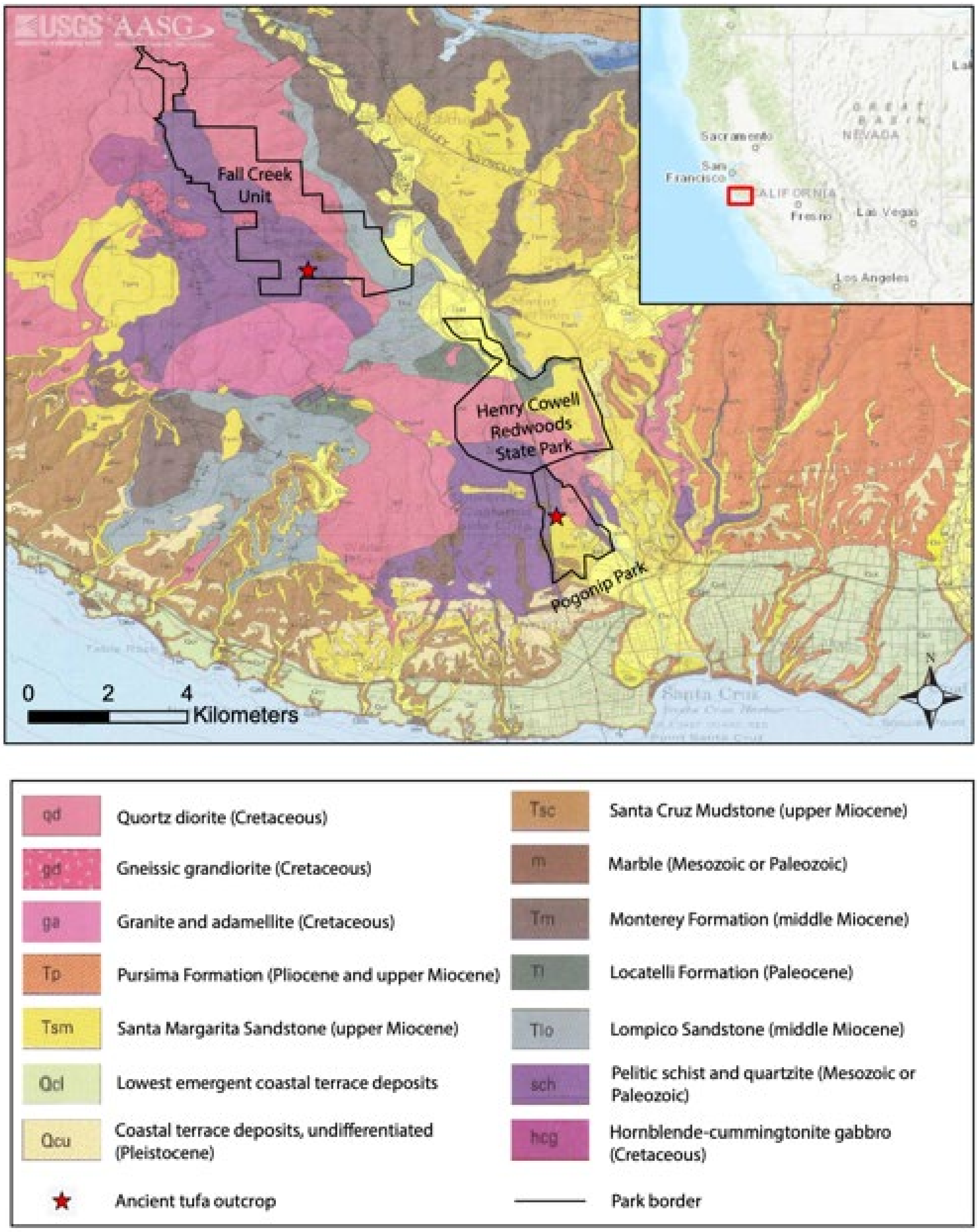

Figure 1. Geologic map of Santa Cruz, CA county, noting areas of Pogonip Park and Henry Cowell State Park. Includes locations of inactive, ancient tufa deposits noted in this study. Map adapted from Brabb, 1989.

1.2 Background

Most tufa studies involve modern or currently-forming and well-preserved Quaternary deposits, which are a common feature of many Mediterranean and other semiarid regions (Pedley, 2009; Arenas et al., 2014). Tufas are commonly used as paleoenvironmental archives and to investigate microbe-mineral interactions (Capezzuoli et al., 2014). The term tufa refers to any freshwater carbonate that forms under ambient temperature conditions and they usually preserve microfossils as well as casts and molds of aquatic and terrestrial plants (Pedley, 2009). While the presence of microorganisms is not necessary for tufa to form, some microphytes can influence tufa deposition (Capezzuoli et al., 2014). In the Santa Cruz region, cyanobacteria and algae (e.g., diatoms) inhabit the spring water and influence the textures and formation of the modern and ancient tufa (e.g. Boelts et al., 2020; Ibarra & Sanon, 2019).

Tufa formation is typically associated with regions that have a limestone component to the bedrock under a range of seasonal environmental conditions (Arenas et al., 2014; Kano et al., 2003; Matsuoka et al., 2001; Andrews & Brasier, 2005; Shiraishi et al., 2010). The principal environmental controls include water temperature, stream velocity, water chemistry, water depth, distance from the spring input, and physiological activity of flora and bacteria (Arenas et al., 2014; Kano et al., 2003; Matsuoka et al., 2001; Andrews & Brasier, 2005). All of these factors combined, along with regional topography (Viles et al., 2007), control the seasonal trends and overall morphologies of tufa deposits (Arenas et al., 2014; Shiraishi et al., 2010) (see Table 1). Seasonal tufa deposition can be represented by mm-scale laminae, which can vary in texture, thickness, and color (Arenas et al., 2014; Arenas & Jones, 2017; Shiraishi et al., 2010).

The temperature of cold springs usually mimics the temporal pattern of the air temperature across seasons (Shiraishi et al., 2008). Therefore, spring water temperature can be reflective of overall climate and season that the region was experiencing at the time of tufa formation (Matsuoka et al., 2001). Moreover, water temperature controls the type of organisms that thrive in the aqueous environment, which can determine whether a particular set of laminae formed biotically or abiotically. For example, *Oocardium stratum*, a green algae, is known to thrive in ambient-temperature spring waters and secretes extracellular polymeric substances (EPS), which induces calcite formation (Ibarra & Sanon, 2019). Spring velocity and turbulence impacts the rate at which tufa can form—high flow velocities and turbulence induces CO_2 degassing from the water, which favors calcite precipitation (Arenas et al., 2014). Photosynthesis by aquatic microorganisms is also thought to have an impact on tufa formation, however its significance is currently disputed (Shiraishi et al. 2008, 2010; Arenas et al. 2014; Spiro & Pentecost, 1991; Andrews & Brasier, 2005).

1.3 Tufa as a Proxy for Paleoclimate

The presence of large, meter-scale ancient tufa accumulations in semi-arid regions is indicative of past episodes of greater groundwater recharge, or past pluvials (Capezzuoli et al., 2014; Ibarra et al., 2015; Viles et al., 2007). Certain facies and erosional features can be indicative of historical changes in water discharge (Arenas et al., 2014; Viles et al., 2007; Capezzuoli et al., 2014). Understanding these past changes in hydroclimate can provide context for how the region's hydroclimate will vary in the future (Ibarra et al., 2015). So far, little investigation has been done on the paleoclimatic significance of tufas in the Santa Cruz region. However, other studies have been conducted in similar climates at comparable latitudes around the world and can be used as a reference when discussing tufa as a proxy for paleohydroclimate in the Santa Cruz region (e.g., Andrews et al., 2000; Andrews & Brasier, 2005; Arenas et al., 2014; Arp et al., 2001; Beverly et al., 2015; Cremaschi et al., 2010; Desouky et al., 2015; Ibarra et al., 2015; Kano et al., 2003; Özkul et al., 2013; Pedley, 2009; Rodríguez-Berriguete & Alonso-Zarza, 2019; Sancho et al., 2015; Sanders et al., 2011; Viles et al., 2007).

1.4 Astrobiological Significance of Tufa

There is strong evidence that tufa-like deposits exist on Mars (Pellicer et al., 2014; Horgan et al., 2020; Niles et al., 2013; Ehlmann et al., 2008; Morris et al., 2010; Michalski & Niles, 2010; Halevy et al., 2011). Although there is currently no evidence that life exists on Mars—now or in the past—certain geologic features on the surface of Mars suggest that the planet previously displayed conditions that would have been conducive to harboring life (McMahon et al., 2018, Cabrol & Grin, 1999; Fassett & Head, 2008; Goudge et al., 2016; Grant et al., 2008; Grotzinger, et al., 2015; Malin & Edgett, 2003; Metz et al., 2009; Moore & Howard, 2005, Horgan et al., 2020; Wordsworth, 2016; Farley et al., 2020). Given previous evidence of Martian carbonate forming under ambient-temperature conditions and fluvial geomorphological features on the surface of Mars (i.e., McMahon et al., 2018, Cabrol & Grin, 1999; Fassett & Head, 2008; Goudge et al., 2016; Grant et al., 2008; Grotzinger, Gupta, et al., 2015; Malin & Edgett, 2003; Metz et al., 2009; Moore & Howard, 2005, Horgan et al., 2020; Wordsworth, 2016; Farley et al., 2020), tufa mounds derived from ambient-temperature, freshwater springs have the potential to serve as analogs for similar landforms on Mars (Pellicer et al., 2014, Rossi et al., 2008; Halevy et al., 2011). Tufas can be an analog for subaerial environments on Mars (Hays et al., 2017; Cady et al., 2003), such as the delta in Jezero Crater.

In the search for traces of life (i.e. biosignatures) in Early Earth deposits or on other planets there is a dearth of unequivocal criteria that distinguishes microfossils and biotically controlled structures from pseudofossils and non-biologically produced structures (Cady et al., 2003; Cady & Noffke, 2009; Dupraz et al., 2009; Grotzinger & Knoll, 1999; Wagstaff & Corsetti, 2010). If microbes did, in fact, exist on Mars we might expect them to be preserved in a similar way to microbes in Earth's rock record (McMahon et al., 2018; Farley et al., 2020). The calcified microbial textures—e.g., stromatolites—found in the tufas from Henry Cowell State Park likely formed under microbial influence and are discernable signs of life that can be identified by current rover technology on Mars, which can photograph features as small as ~0.5 mm (Williford et al., 2018). Investigating these textures will help inform sample prioritization on Mars and other rocky planets. Using a multiscale biosignature analysis (*sensu* Ibarra & Corsetti, 2016), of modern and ancient tufa from Henry Cowell State Park, I will distinguish morphological biosignatures at scales that could be detected by current rover technology.

2. Geologic Setting of the Santa Cruz Region

The Santa Cruz region—roughly 80 miles south of San Francisco State University—experiences an arid Mediterranean climate (Adam et al., 1981) and, on average, receives 65 cm of precipitation annually with an average annual temperature of 14 degrees Celsius (Lyle et al., 2010). On longer timescales, the Santa Cruz region fluctuates between wet and dry periods—correlating with glacial and interglacial cycles—and it is likely that there was an increase in rainfall in central California during the most recent interglacial wet period (12,500 to 4,500 years ago) (Lyle et al., 2012). The study sites are located between the San Andreas Fault (to the east) and the San Gregorio and Sur-Nacimiento Faults (to the west) (*University of California…*, 2005). Moreover, the region is situated on the Salinian block, which presents a basement complex of old metamorphic rocks and more recent granitic rocks (Lee, 1992) that is being uplifted and pushed northward by the San Andreas Fault (Anderson & Menking, 1994). Santa Margarita sandstone and Santa Cruz mudstone overlay the basement complex, but much of these Formations have been eroded in the vicinity of the study sites (see Fig. 1) (Lee, 1992). The sites that were investigated in this study, Pogonip Park and Henry Cowell State Park, are located on the southwestern part of Ben Lomond Mountain and are part of the greater Santa Cruz Mountain range (*University of California…*, 2005).

The limestone marble bedrock that underlies much of the region is primarily composed of calcite and comprises the region's karst system (*University of California…*, 2005). The karst system contains extensive solution cavities, which store and transport groundwater (*University of California…*, 2005). The known depth to groundwater in the marble aquifer system is variable—ranging from approximately 30 to 90 meters below the ground surface (*University of*

California…, 2005). This variability in depth would likely contribute to the changes in the rates of discharge among the region's karst springs.

2.1 Henry Cowell State Park

Henry Cowell State Park is located approximately seven miles north of the city of Santa Cruz (California State Parks, 2011). Geologically, the southern part of the park contains schist and granite, while the northern part consists of sandstone and mudstone as well as quartz-diorite (Brabb, 1989; California State Parks, 2011). Given its close proximity to Ben Lomond Mountain—part of the greater Santa Cruz Mountains—the park displays a mountainous topography. The park is divided into two units, separated by the city of Felton, CA: Henry Cowell Redwoods State Park and the Fall Creek unit. Our research site is located in the Fall Creek unit (Fig. 1), which encompasses 2,390 acres of land as well as the entire Fall Creek watershed (California State Parks, 2011). We investigated an inactive, ancient tufa mound and modern tufas. The modern and ancient deposits are on Mesozoic or Paleozoic pelitic schist and quartzite, part of the Salinian block (Brabb, 1989). Ringtail Creek, the water source of interest in this investigation, is one of several streams in the Fall Creek watershed and extends for 1.26 kilometers ("Ringtail Creek"). The creek is actively forming tufa today, however the rates of tufa formation are currently unknown.

2.2 Pogonip Park

Just north of the University of California Santa Cruz campus and two miles inland from the Pacific Ocean is the 614 acres that composes Pogonip Park (Lee, 1992). Pogonip Park is situated on one of the ~5 marine terraces in the region and topographically consists of steep slopes and gullies as well as flat meadows and terraces (Lee, 1992)—although less mountainous compared to Henry Cowell State Park. The marine terraces are mostly mudstone and are part of the Monterey Formation (Bradely, 1957). The rocks that compose Pogonip Park include: marble, schist, quartz-diorite, Santa Margarita sandstone and Santa Cruz mudstone (Lee, 1992). Karst topography is evident in this area due to the presence of limestone and marble (*University of California…,* 2005). It is thought that much of the surface water drains into the karst underground system, is held in a fractured aquifer system, and is then discharged into springs (*University of California…*, 2005). The spring that formed the carbonate outcrop of interest in Pogonip Park would have likely been a product of the groundwater system described above, and, perhaps, Ringtail Creek is a product of a similar system.

The ancient tufa outcrop described in this study sits along the Spring Trail in Pogonip Park and is exposed along the trail for 15 meters. Its thickness varies along the path from 2.5 meters to the east and 4 meters to the west and the buildup of carbonate displays a wedge shape (Ibarra & Sanon, 2019). Similar to the outcrop in Henry Cowell State Park, determining the full extent of this outcrop is difficult given the amount of topsoil and vegetation that covers it. The mound's exposed facies display porous textures and weakly bedded macrostructures (Fig. 2) (Ibarra & Sanon, 2019). It is likely that the mound was altered by humans when the trail was built, therefore making it difficult to place it in a depositional model. However, given the description from Ibarra and Sanon 2019, the mound likely represents a perched, inactive tufa model. Furthermore, while an ephemeral spring is relatively nearby (~100 meters) there is currently no evidence that the spring is related to the mound (Ibarra & Sanon, 2019).

Figure 2. Exposed Tufa Outcrop in Pogonip Park

3. Methods

3.1 Sample Collection

3.1.1 Pogonip Park

The paleohydroclimate encoded in the tufa deposits from Pogonip Park was assessed by collecting three tufa cores (each 25 mm in diameter and up to ~60 cm long) of the exposed outcrop (Fig. 2). Two cores were collected for luminescence dating using a Shaw portable core drill. Core PN was collected roughly 80 cm from the base of the section (Fig. 3B). Core P1 was collected 10 cm from the base of the section approximately 2 m north from core PN. Upon collection, the two cores were immediately transferred into photographic bags while in the field, and stored in dark conditions until their subsequent luminescence analysis at the Illinois State Geological Survey. Prior to analyses, core PN was slabbed longitudinally using amber lighting. Half of the core (PN) was repackaged in light-sensitive bags for IRSL analyses and the second half was scanned on a flat-bed scanner for further textural analyses. The third core was sliced in half vertically using a wet tile saw, and each half was examined petrographically at SFSU.

3.1.2 Henry Cowell State Park

This study used one core and nine decimeter-scale samples from Henry Cowell State Park. Of the nine samples, five were from the perched, inactive tufa mound and four were collected from the carpeted modern tufas. Collection of decimeter-scale hand samples and core from the ancient mound was limited by the steep topography of the area. All samples were slabbed and scanned on a high-resolution flat bed scanner. Cross sections were subsequently made into thin sections—nine from the ancient mound and five from the modern tufas. Field photos, decimeter-scale hand samples, cross sections, and thin sections were used for petrographic analysis. The core from Henry Cowell (25 cm) was extracted horizontally approximately 8 cm from the base of the mound, below the tufa curtain (Fig. 3A). The core was cut in half length-wise; half was scanned on a flat-bed scanner and two samples (each ~2 cm in length) were prepared for palynological analyses at Global GeoLab Limited. Fragments of charcoal from the insoluble residue of these two samples were dated using radiocarbon.

3.2 Radiocarbon

Five Accelerator Mass Spectrometry (AMS) ^{14}C dates were obtained from carbonate and organic fragments collected from the ancient tufa mound and modern tufa in Henry Cowell State Park and the ancient tufa mound in Pogonip Park. One carbonate fragment of the Pogonip core that was selected for ^{14}C analysis lacked organics and therefore the carbonate was dated instead. Two ~6 cm fragments (the most innermost section and the furthest out section) from the Henry Cowell core contained an abundance of organics (pollen/charcoal), which underwent ^{14}C analysis (Fig. 3A). The associated carbonate from the innermost part of the core was also dated (Fig. 3A). A carbonate sample from the carpeted, modern tufas adjacent to the current path of the carbonate spring contained ample charcoal. We hand-picked the largest charcoal piece (measuring at 2 cm^2) for ^{14}C analysis (Fig. 3C). Samples were sent to the UC Irvine Keck Laboratory for radiocarbon analysis.

Figure 3. Locations of 'Dark Cores' and Charcoal Sample

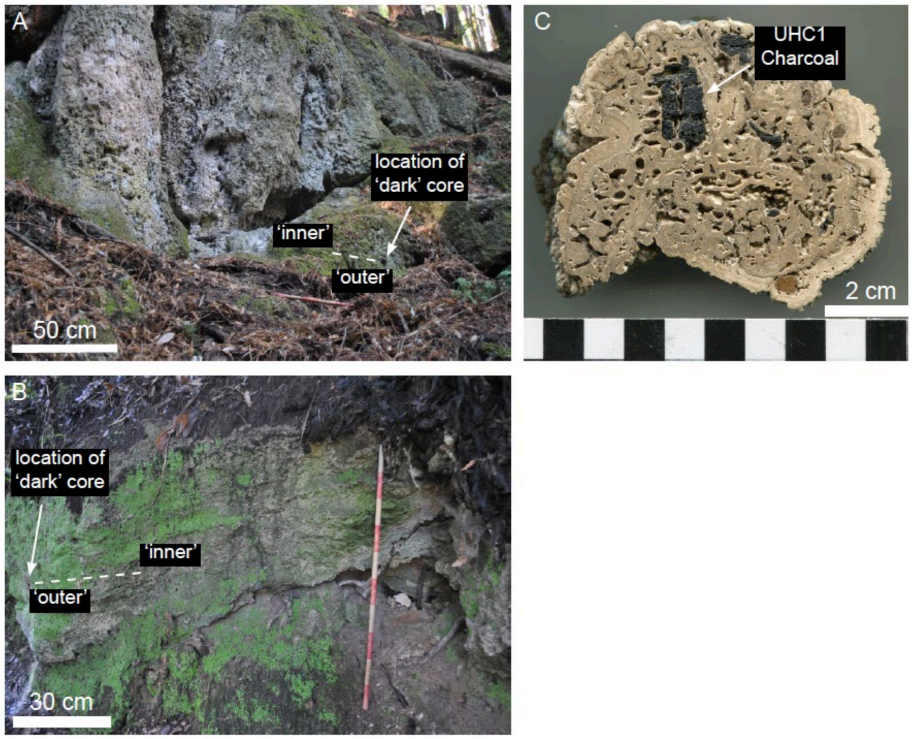

Figure 3. (A) Location of 'dark core' collected from Henry Cowell State Park for IRSL and radiocarbon dating. (B) Location of 'dark core' collected from Pogonip Park for IRSL and radiocarbon dating. (C) Piece of charcoal for radiocarbon dating collected from sample UHC1. Sample collected from Henry Cowell State Park.

3.3 Infra-Red Stimulated Luminescence (IRSL)

Depositional chronology was constrained by luminescence dating (Aitken, 1998; Rhodes, 2011). Luminescence dating is based on the principle that quartz and orthoclase minerals (among others) have an intrinsic property of recording ambient energy, released through natural radioactivity. This clock is easily reset by a short exposure to sunlight (minutes to hours). Buried, these minerals will record the ambient energy, whenever radioisotopes of uranium 238, thorium 232, and potassium 40 experience a radioactive decay. For this project, we use IRSL of K-feldspar minerals since tufa primarily consists of carbonates, while silicate minerals are relatively sparse. There is an additional focus on K-feldspar rather than quartz because K-feldspar emits a stronger luminescence signal (by a few orders of magnitude). Utilizing quartz would severely limit the amount of measurements possible on a core, but we were not limited with K-feldspar. K-feldspar minerals also have a significant internal source of radioactivity (from ^{40}K). The distribution of radioactive elements in tufa is sparse and heterogenous, therefore, having an internal source of radioactivity tempers this external influence (Ibarra et al., 2015).

3.4 Multiscale Observations

The facies of the 14 decimeter-scale tufa samples collected from Henry Cowell State Park were analyzed and compared at multiple spatial scales. These scales include micro- (millimeters or less), meso- (centimeters), macro- (decimeters), and mega- (meters or more) (Fig. 4). Microscale observations were made using petrographic analysis of thin sections. Meso- and macroscale observations were made via photomosaics of thin sections and petrography of hand samples (both *in situ* and in cross-section). Lastly, mega-scale observations were made while surveying the deposits in the field. The internal and external (surface) facies were considered when determining the potential processes, or controls, that influenced their formation (Table 1).

Figure 4. Lateral Comparative Analysis

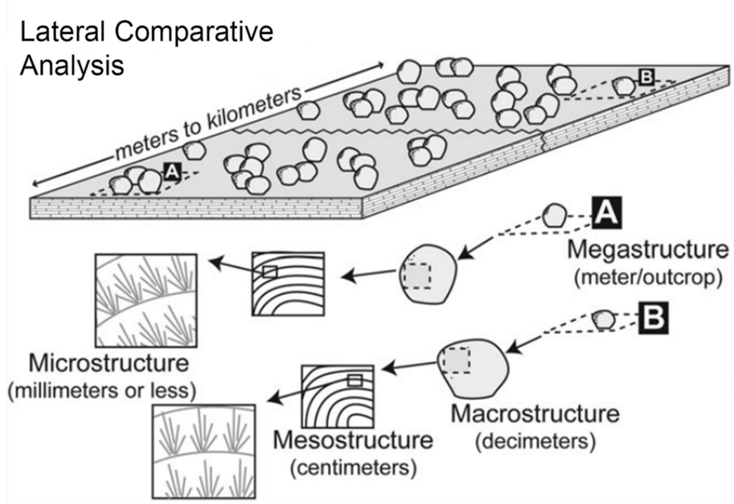

Figure 4. Lateral comparative and multiscale analysis of tufa. Modified from Ibarra & Corsetti, 2016.

Table 1. Processes of Control on Tufa Morphology

Scale of control		*Morphogenesis (inorganic)*	*Biogenesis (organic)*	*Diagenesis (postdeposition)*
Local	µm	Crystal growth; stream water chemistry	Microbes	Cementation, dissolution, precipitation; replacement/inversion; micritization
	mm	Crystal growth; sedimentation	Microbes; passively altering textures; actively inducing precipitation	Cementation; dissolution; precipitation
	cm	Crystal growth; cement growth; sedimentation	Biofilms; microbial mats; trapping and binding of sediment	Cement, dissolution, precipitation
	m	Spring outflow; lateral gradients of (physical, chemical) flow; turbulence	Biofilms; microbial mats; microbial chemical/nutrient recycling	Soft-sediment deformation; burial; slumping; desiccation; displacive growth by evaporites
Nonlocal	km	Climate; seasonality; water level/depth; water chemistry; nutrient supply	Dispersal of microbial communities (controlled by factors in km-scale morphogenesis)	Burial; compaction; tectonic deformation

Table 1. Potential processes of control on tufa morphology in Henry Cowell State Park at various scales (modified from Ibarra & Corsetti, 2016).

4. Results

4.1 Spring Carbonate Facies

4.1.1 Perched Carbonates

The ancient tufa mound (> 1,000 years old) in Henry Cowell State Park is roughly 4 meters thick and spans a length of around 4.5 meters (Fig. 5A). It sits roughly 15 meters south of the current path of Ringtail Creek. The steep topography of the area, along with the vegetation and topsoil that sits above the mound, makes it difficult to know its full extent and macrofacies (e.g. stepped terraces). The mound is wedged into the side of a steep slope and its southern unit resembles waterfall facies with small curtain-like features towards its base (Pedley et al., 2003) (Fig. 5B). The southern part of the mound that was accessible for sample collection displays drippy speleothems (Fig. 7A). Moving north along the face of the outcrop, the surficial macrostructure becomes “spikey” followed by a “popcorn” fabric, partially covered by a blue fungus (Fig. 5B).

Carbonate samples collected from the perched tufa contain distinct, irregular banding at the mesoscale (approximately 0.2-0.5 mm in thickness). The mm-scale bands alternate between sparry and micritic laminae. The texture of carbonates is defined by vuggy, mesoscopic pore space. At a microscopic scale, carbonate fabrics are primarily composed of micrite, microspar, and spar—all of which are irregularly distributed (Figs. 6 & 7). Most samples contained bands of microalgal fossil remains—specifically *Oocardium stratum* and diatoms. *Oocardium* was found in bands of spar, while diatoms were typically present in micritic fabrics and pore space (Figs. 6 & 7). Furthermore, diatoms and diatom frustule molds (~50-100 µm in length) as well as well-preserved coccoid biota (~15 µm in diameter) co-exist in all diatom-bearing samples (Fig. 7).

Figure 5. Ancient Tufa Outcrop in Henry Cowell State Park

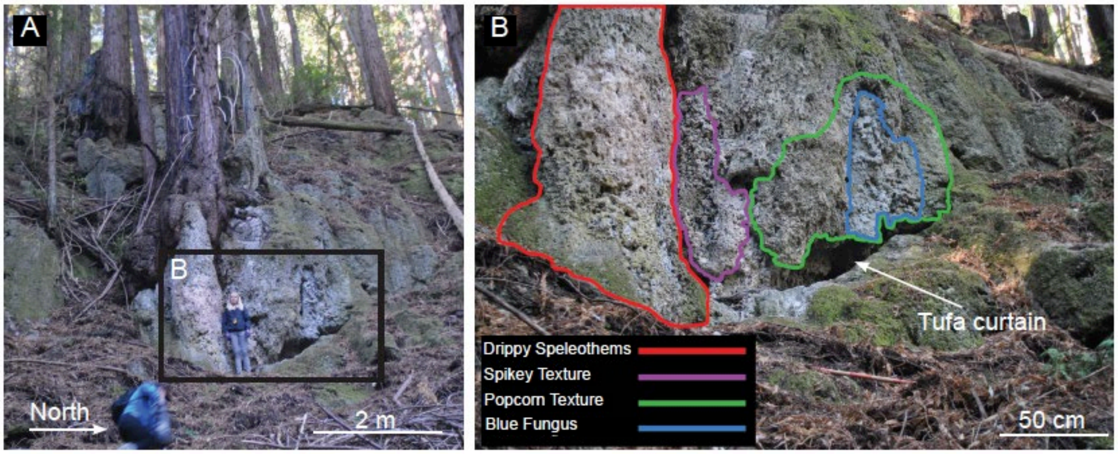

Figure 5. (A) Perched, inactive springline carbonate mound. Human for scale. (B) Surficial macrostructures of accessible tufa mound. (C) Drippy speleothems and tufa curtain of the southern portion of the tufa mound. Hammer for scale.

Figure 6. Internal Facies of Perched Carbonates at Multiple Scales

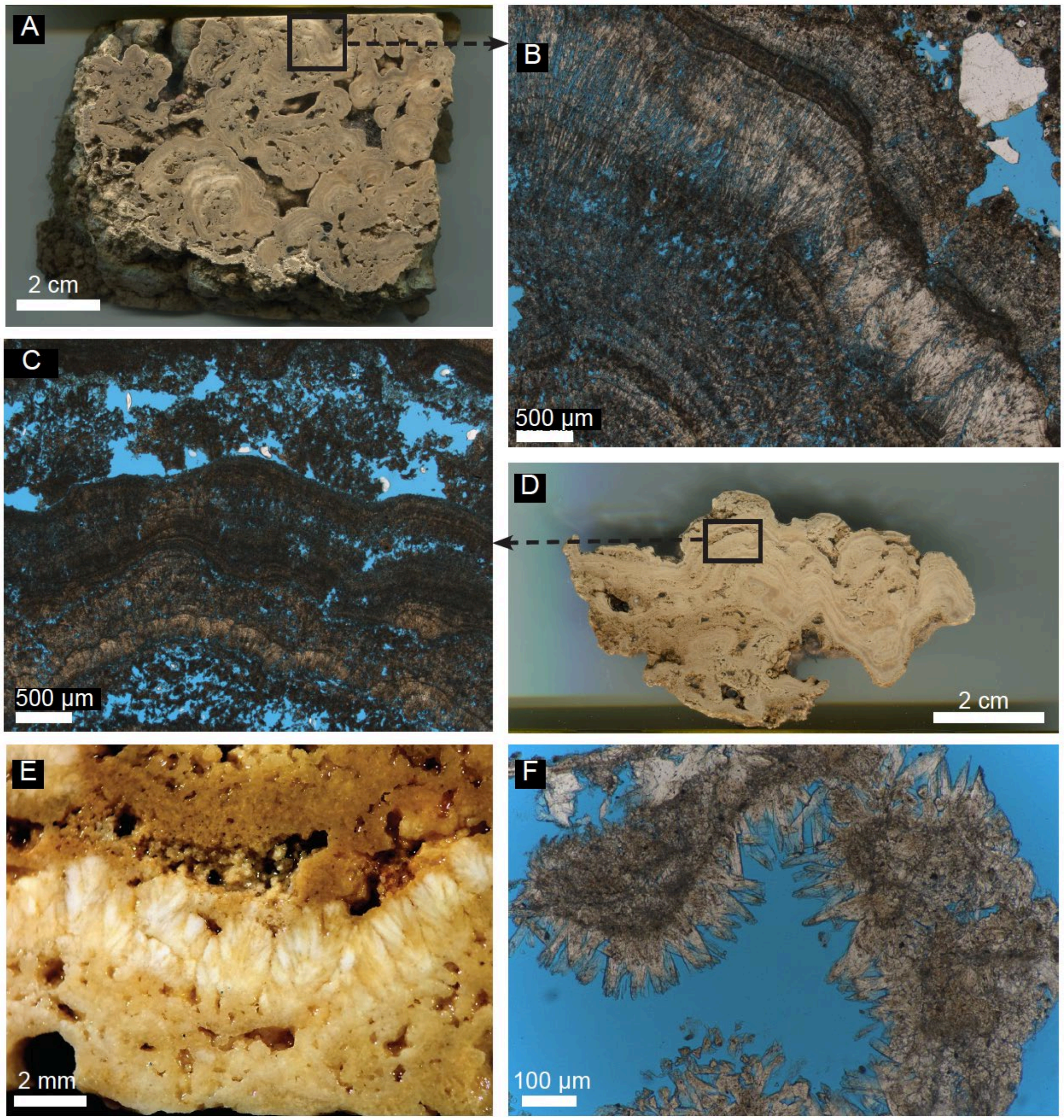

Figure 6. (A) Cross-section of carbonate sample. Depicts vuggy pore space and banding of Oocardium. Sample collected from Henry Cowell State Park (B) Lamina of fossilized Oocardium. (C) Banding of fossilized Oocardium (sparry, dense laminae) altering between porous, micritic laminae. Sample collected from Henry Cowell State Park (D) Cross-section of carbonate referenced in (C). (E) Dendritic mm-scale shrubs in a prominent band of polished carbonate core collected from Pogonip Park (modified from Ibarra & Sanon, 2019). (F) Dog-toothed spar growing in pore space.

Figure 7. Facies of Perched Carbonates (Drippy Speleothems)

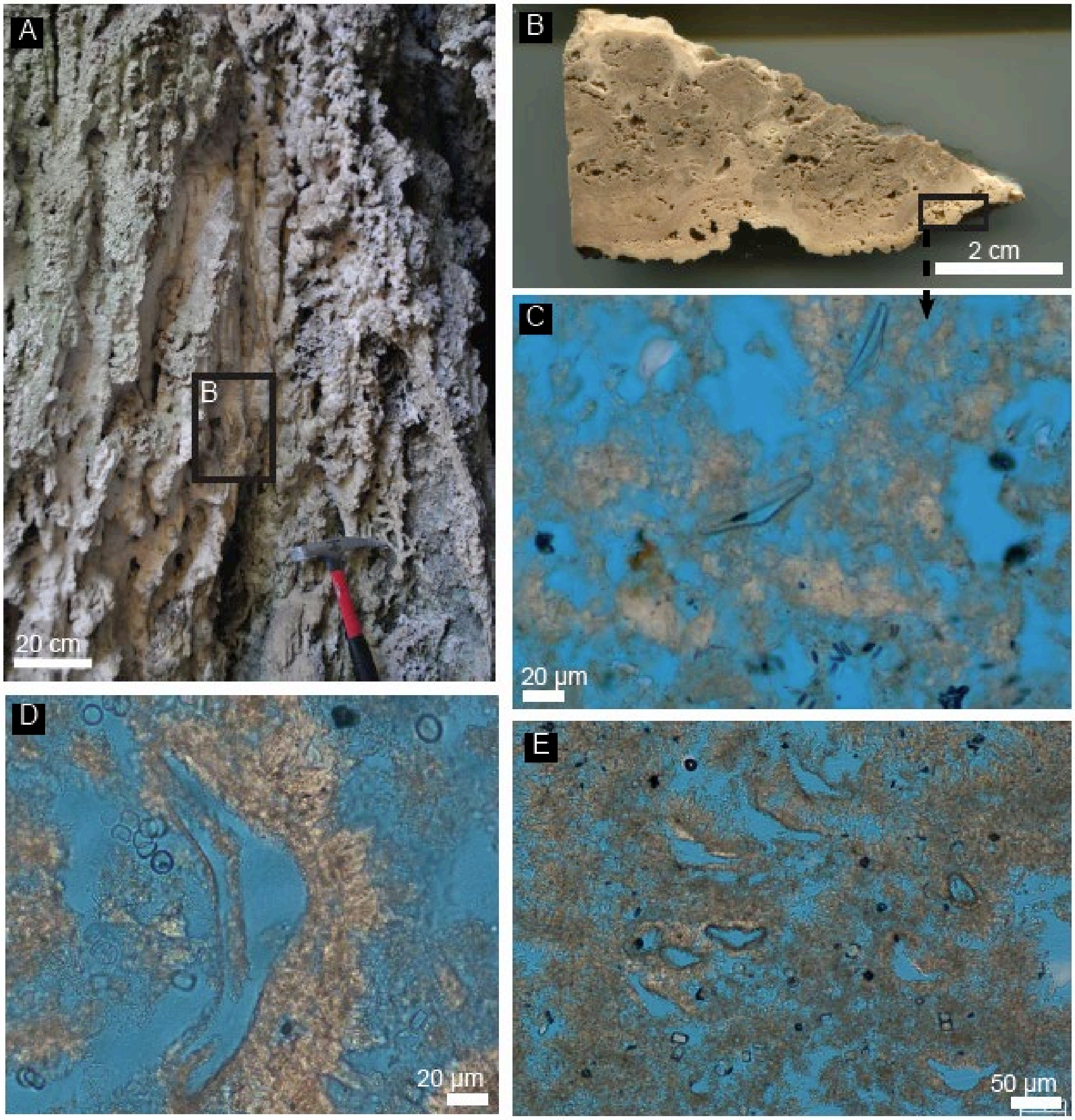

Figure 7. (A) Drippy speleothem morphology of tufa outcrop. Location of where (B) was collected. (B) End piece of speleothem in cross-section. (C) Fossilized pennate diatoms in micritic fabric. Preserved in the crust of the speleothem. (D) Mold of diatom frustule encrusted with isopachous calcite. Coccoid biota present around frustule mold. (E) Molds of diatom frustules and coccoid biota at a slightly larger scale.

4.1.2 Fluvial Carbonates

Upstream from the ancient tufa mound in Henry Cowell State Park, immersed in Ringtail Creek, were modern tufas (< 1,000 years old). We examined an area spanning approximately 6 square meters that exhibits paludal/channel and stromatolitic facies (Fig. 8, Pedley, 2009), which was located approximately 30 meters from the spring source. At the macroscale, the carbonates contained decimeter-scale domes, whose surface displayed a “cauliflower”-like fabric (Fig. 8B, 9). The decimeter-scale domes (Fig. 8B) as well as the cauliflower-like textures were internally laminated and hence stromatolitic (Figs. 9 & 10). The stromatolitic laminations alternated between bands of spar and micrite, but the overall fabric were dominated by irregularly distributed micrite, microspar, and spar with poor lateral continuity between adjacent decimeter-scale mounds. Most samples contained a relatively high abundance of clastic material such as schist, granite, and charcoal clasts (Fig. 9 & 10). Well-laminated and banded crust surrounded the inner clastic area, with calcite bands ranging in 0.1-1 mm in thickness.

Figure 8. Fluvial Carbonates In Situ from Henry Cowell State Park

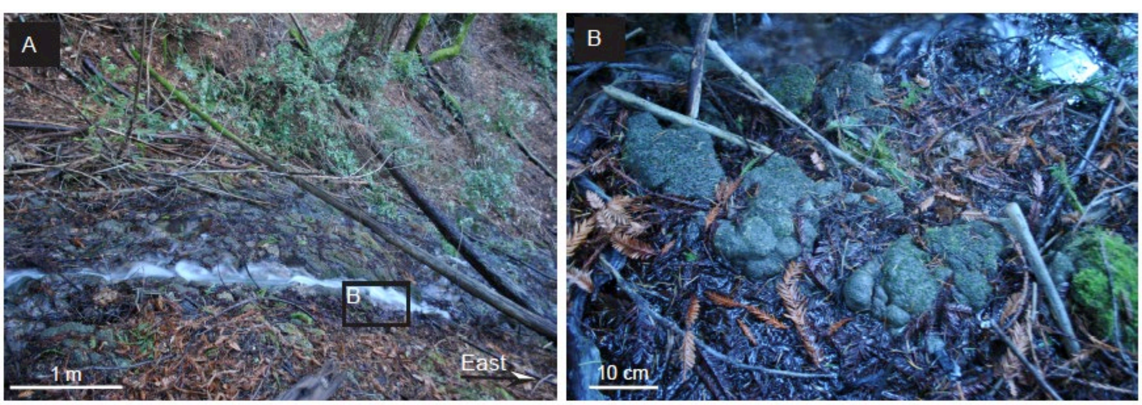

Figure 8. (A) 6 square meter study area of fluvial tufas carpeted in and around Ringtail Creek. (B) Cauliflower-like texture of fluvial tufas in situ.

Figure 9. Multiscale Facies Analysis of Fluvial Carbonates

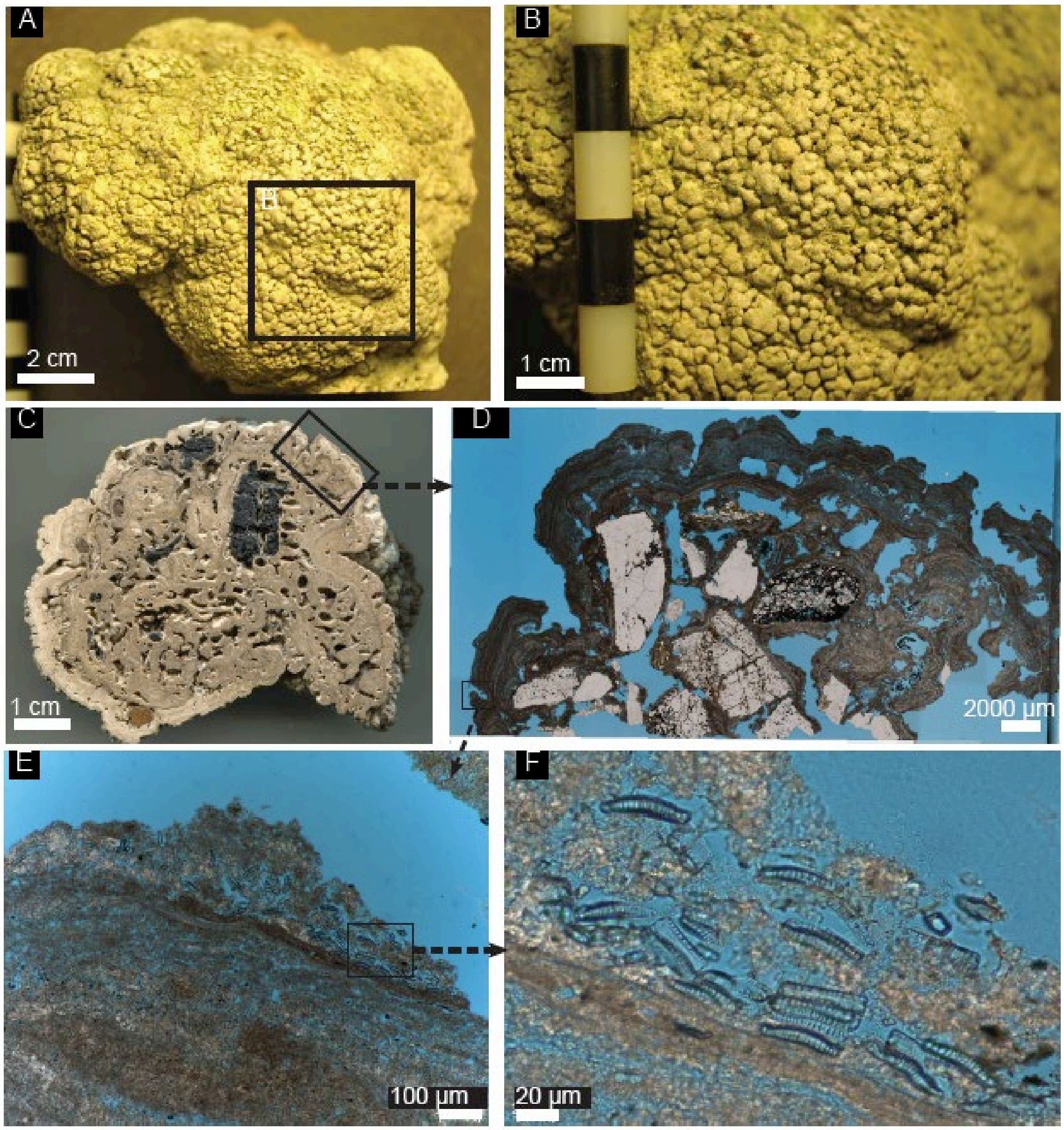

Figure 9. (A-B) Cauliflower-like outer fabric at macro- and meso- scales respectively. (C) Sample in cross-section. (D) Piece sample in thin section. Internal stromatolitic fabrics show upward direction. (E-F) Pennate diatoms preserved in crust.

One sample collected close to the spring path contained horizontally oriented diatoms (~20 µm in length) in its outer crust (Fig. 9) and thus on the surface of the cauliflower-like fabric. Moreover, porous fabrics contained filamentous morphologies measuring ~8-10 µm in diameter (Fig. 9). There were three prominent internal textures that comprise this sample: dense micrite, pores, and sparry areas (Fig. 9). The presence of diatoms in the crust of the other submerged or partially submerged samples could not be confirmed because their outer layers were not mounted in thin section.

Another sample that was collected several meters away from the spring contained fossilized *Oocardium* and relatively continuous, distinct banding (Fig. 10). The internal and external morphology of this sample differed from those collected near the spring path. The banding (>0.1-0.3 mm in thickness) alternated between light and dark as well as dense and porous textures. Vuggy porosity is observed throughout this sample. More porous textures and cylindrical molds are observed towards the bottom of the sample (Fig. 10). This, and the subtle domal shapes of certain laminae, indicated an up direction (Fig. 10). Overall, this sample most closely resembled those collected from the perched outcrop.

Figure 10. Facies of Distal Fluvial Carbonate at Multiple Scales

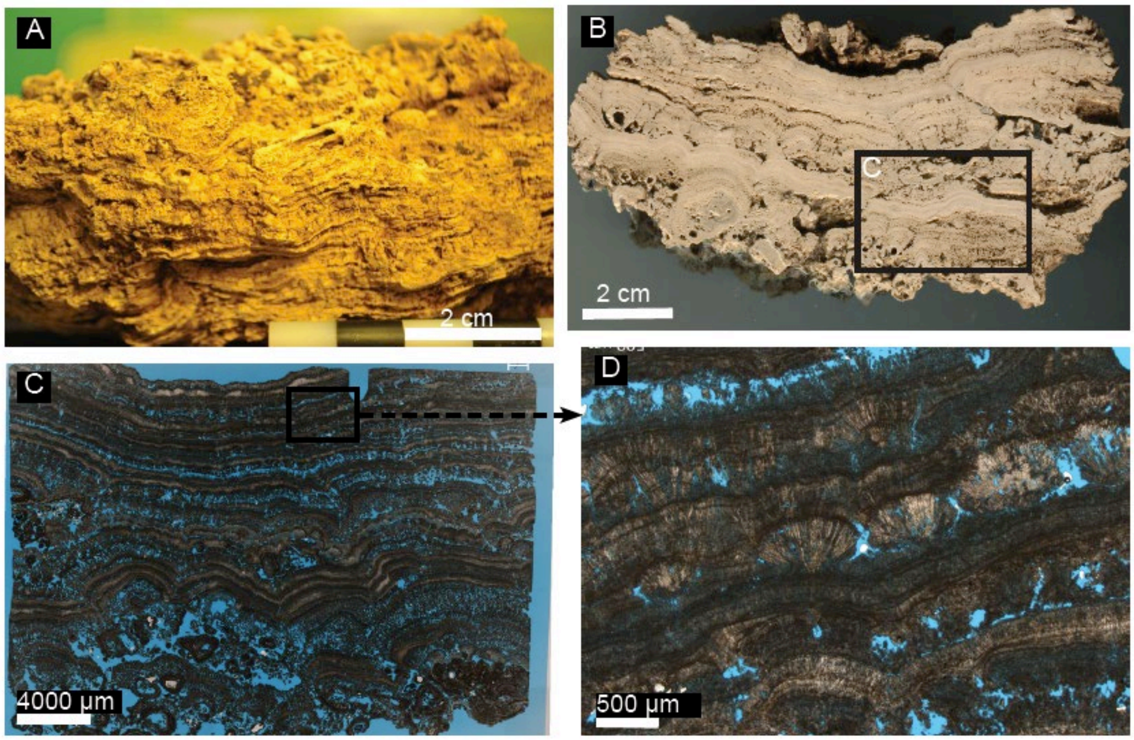

Figure 10. Multiscale facies of carbonate collected distal from the spring path and fluvial carbonates in Henry Cowell State Park. (A) Outer layered morphology. (B) Sample in cross-section. (C) Photomosaic image of thin section. (D) Alternating layers of fossilized Oocardium and porous, micritic textures.

4.2 Ages

Table 2. ^{14}C age data for carbonate and organics from the tufa deposits

UCIAMS	Sample name	Location	^{14}C age (BP)	±	2 sigma range [a]	Age Cy BP [a]
240214	UHC1-charcoal	Henry Cowell Fluvial	920	20	840-911	853
240216	HC3-residue	Henry Cowell Perched	5380	20	6227-6279	6206
240217	HC1-residue	Henry Cowell Perched	7170	20	7944-8017	7986
240222	HC1-carb	Henry Cowell Perched	3675	20	3963-4088	4030
240223	P0-carb	Pogonip	13965	35	16851-17092	17000

Table 2. [a]Calibrated age on IntCAL Reimer et al., 2020

Table 3. Luminescence results for each of the two "dark cores"

ISGS code	Sample	Mineral	Grain Size (µm)	Equivalent dose (Gy)	Dose rate (Gy/ka)	Age (ka)
684	P1	K-Feldspar	63 - 100	6.6 ± 0.9	0.54 ± 0.02	12.2 ± 1.8
709	Pogonip "N"	K-Feldspar	40 - 63	11.5 ± 0.8	0.45 ± 0.02	25.6 ± 2.2

4.2.1 Radiocarbon

A charcoal piece from a tufa sample UHC1 from the fluvial carbonates at Henry Cowell State Park has a calibrated age range of 840-911 cy BP (2σ) (Reimer et al., 2020). The data was calibrated on CALIB 8.2 (Stuivier et al., 2021) using the calibration curve INTCAL20 for non-marine samples. Organic residue (microscopic charcoal fragments) from the Henry Cowell core have calibrated ages of 6,206 and 7,986 cy BP and corroborate the stratigraphic order we would expect given the inferred paleoflow direction at the time the tufa mound was deposited. The calibrated age of a carbonate sample (HC1-carb) from the core at Henry Cowell State Park is 4,030 cy BP. The calibrated age of a carbonate sample from the third core collected at Pogonip Park (innermost piece) is 17,000 cy BP. The ^{14}C ages of carbonate, however, likely reflect mixing of soil derived CO_2 with old bedrock carbon and are therefore not considered meaningful here for temporal reconstruction—even if they fall within the range expected based on the ^{14}C results at Henry Cowell State Park and the luminescence results (described below) for Pogonip Park.

4.2.2 IRSL

Two IRSL measurements were obtained from the cores collected at Pogonip Park (one age measurement for each core) (Table 3). Sample P1 has an age range of 12.2 ± 1.8 ka. A radial plot illustrating the uncertainty in the age measurement is shown in Appendix A. The 12.2 ± 1.8 ka reported here are for K-spar grains whose ages fall within the 2σ range (Appendix A). After the fading correction (Huntley and Lamothe, 2001), each circle on the radial plot represents the age and uncertainty, for a single aliquot. The age is read on the arc axis, by drawing a straight line from (0, 0), passing through a circle and intersecting the radial axis (log scale). The (0, 0) coordinate corresponds to a 0 standardized estimate (y-axis) and 0 precision (x-axis). The uncertainty is read on the horizontal axis, by drawing a perpendicular line reaching a circle. Hence, two aliquots, having the same age, but with different uncertainty, will lay on the same straight line (from (0, 0) to the radial axis). The aliquot with the smaller uncertainty (higher precision) will be closer to the arc. Values (filled circles) within the light grey shaded band are consistent (at 2σ) with the weighted mean (Central Age Model). A cluster of aliquots within this shaded band expresses confidence that we have a population of grains consistent with a single age. It is noted that there is a cluster of ages slightly outside the 2σ range at ~6 ka and another at ~22 ka (Appendix A).

Sample PN has an age range of 25.6 ± 2.2 ka, however, it is noted that the IRSL decay curve between the natural and the laboratory induced dose (regen) shows a pronounced change (see Appendix A) rendering this age unreliable. The smaller size fraction of K-spar grains detected in the core PN (Table 3) likely contributed to the differences in the decay curves. It is important to note that due to the high lateral morphological variability and erosional nature of tufa deposition, it is likely that these ages do not reflect the only tufa growth periods at this site and/or that we did not sample other potential zones of paleoflow.

5. Discussion

5.1 Comparison to Other Regional Paleoclimate Proxies

Quaternary terrestrial records of paleoclimate are limited in the Santa Cruz, CA region. Arguably the most robust terrestrial proxy of paleoclimate in the region is the pollen record (Rypins et al., 1989, Adam et al., 1981). Rypins et al., (1989) used pollen collected from Point Reyes, CA (210 km north of Santa Cruz) to model past shifts in plant ecology. Between 12 ka and 10 ka, the area was dominated by *Abies* (fir) and *Pseudotsuga* (Douglas fir), implying cooler and wetter conditions. Adam et al., (1981) drew slightly contradicting conclusions from pollen and radiocarbon dating of plant debris collected from Clear Lake, CA (280 km north of Santa Cruz). Their results indicate a transition from cooler and wetter conditions to warmer, modern-day climate between 15 ka and 10.4 ka due to the gradual increase in *Quercus* (oak) and decrease in *Pinus* (pine) during that time period. The difference in timing between Rypins et al., (1989) and Adam et al., (1981) could be attributed to the differing climates between Point Reyes, CA and Clear Lake, CA—where Point Reyes is coastal and experiences relatively cooler summers than Clear Lake, which is further inland. Reneau et al., (1986) collected radiocarbon dates of charcoal from basal colluvium in hollows in Marin County, CA (130 km north of Santa Cruz) to model past landslide events. Such erosional events are thought to be climatically controlled and/or attributed to changes in vegetation. This study found a higher frequency of landslides between 11 ka and 9 ka, indicating heavier rainfall during this time. Another terrestrial record that warrants comparison involves stable isotope analysis and U-series dating of stalagmites from Moaning Cave, California (Oster et al., 2009), which suggests an increase in rainfall from 12.4 ka to 9.6 ka. However, it should be noted that this study is not proximal to the Santa Cruz region and is more widely applicable to the broader central California/central Sierra Nevada region. The most proximal terrestrial record to our sites is that of a speleothem (stalagmite) from White Moon Cave, CA (Oster et al., 2017). The White Moon Cave record indicates coastal California experienced an increase in effective moisture at 8.2 ka.

The marine sediments off the California coast also include pollen data. Lyle et al., 2010 collected pollen and oxygen isotope data from deep-sea cores at ODP site 1018 (75 km west of Santa Cruz, CA). Their results reveal a relatively low abundance of herbs, grasses, and shrubs with a high abundance of forest communities (alder, oak, and redwood) from 13 ka to 5 ka, signaling wetter conditions in the region at the time. Benthic foraminiferal oxygen isotope values were used to corroborate their age model. The results from Gardner et al., (1988) aligns with the age model from Lyle et al., (2010). Pollen collected from a core that was located approximately 100 km west of the mouth of the Russian River shows that *Alnus* (alders) started to increase in abundance at around 16 ka and declined at 7 ka (Gardner et al., 1988). This is significant because alders favor colder and wetter climates. Gardner et al., (1988)'s findings placed the climate in "disequilibrium" from 15 ka to 5 ka, and a wet event could have occurred within that time frame as is supported by the pollen data.

Although these studies, and others (e.g., Lyle et al., 2001; Heusser & Shackleton, 1979), have found correlations between onshore and offshore climate, none of the proxies noted in Table 4 are directly tied to hydroclimate, making the tufas in Santa Cruz, CA a particularly valuable addition to the region's paleoclimate record. All records mentioned, however, point to the same broad trend: a wetter and colder climate during the Pleistocene through the Pleistocene-

Holocene transition and then a long-term drying conditions up to today. The tufa ages support higher groundwater discharge and therefore heavier rainfall (i.e., a pluvial) during the late Pleistocene to Pleistocene-Holocene transition (~6-8 ka), thus generally agreeing with other regional proxies of paleoclimate. The ages of the tufa correspond most closely with the terrestrial records mentioned, which may reflect the differing sensitivities between proxies and depositional settings. Lastly, pollen has been collected from the cores from each site in Santa Cruz. However, their ages and classification has yet to be determined (see Future Work).

Table 4. Timings of Region's Most Recent Wet Event with Corresponding Studies and Proxies

Source	Proxy	Timing of wet event
Lyle et al., 2010	Pollen and benthic oxygen isotopes	13 ka to 5 ka
Reneau et al., 1986	Radiocarbon analysis of charcoal from basal colluvium in 11 California hallows	15 ka to 9 ka
Oster et al., 2017	Carbon and oxygen isotope analysis and U-series dating of stalagmite cores	8.6 ka to 6.9 ka
Rypins et al., 1989	Pollen and radiocarbon dating	12 ka to 9.4 ka
Adam et al., 1981	Pollen and radiocarbon dating	15 ka to 10.4 ka
Gardner et al., 1988	Pollen	16 ka to 7 ka
Oster et al., 2009	Carbon and oxygen isotope analysis and U-series dating of stalagmite cores	11.6 ka to 9.6 ka

5.2 Facies Interpretations

The geomorphological differences of the perched and fluvial tufa in Henry Cowell State Park imply that they formed during different depositional periods. This is also supported by the differing ages of the ancient mound and fluvial tufas. Given the heightened altitude of the perched tufa, it likely formed at a time when the water table was higher than its modern level (e.g., Ibarra et al., 2015; Domínguez-Villar et al., 2011); the presence of spring tufas at different elevations in similar settings can be indicative of shifts in water table levels (Domínguez-Villar et al., 2011). In addition, the path of the spring likely shifted westward compared to today. Thin section analyses indicate the perched tufa experienced some extent of meteoric dissolution and cementation given its well-lithified texture and vuggy porosity (Fig. 6A, D, 7B). This could indicate that they formed in the vadose zone (Ibarra et al., 2015) and/or experienced increased outflow (Martín-Algarra et al., 2003). Furthermore, the presence of dog-toothed spar growing into the pore space (Fig. 6F) indicates several dissolution events—further implying previous wetter conditions.

Samples collected at the base of the mound contain distinct seasonal banding that alternate between *Oocardium*-rich spar and micrite (Fig. 6A-D). Samples collected from higher parts of the mound and in or around the tufa curtain area also contain laminations but lack *Oocardium*. Rather, these samples are rich in diatoms (Fig. 7), revealing potential differing water characteristics (e.g., flow) between different parts of the mound. Shapes resembling partially or entirely dissolved diatom frustules (Fig. 7D-E)—some with spar growing outwards from the mold (Fig. 7D)—imply dissolution and possible silica recycling. While all samples from the perched tufa displayed seasonal patterns (see Seasonal Patterns), the differences in algae between its base and curtain is likely a reflection of differences in stream velocity and/or water chemistry during carbonate deposition at the different sites.

The geomorphic differences observed in the fluvial deposits—high abundance of clastic material and fabrics that are relatively unaltered from dissolution—points to a depositional setting that reflects recent tufa growth under present conditions. The lack of *Oocardium*—with the exception of the sample found adjacent to the stream path—also signals that the spring outflow has decreased over the last 10,000 years. The modern water temperature is within the favorable range for *Oocardium* growth (9-13º C), so stream velocity, or water chemistry, is likely the main factor attributable to its absence in the fluvial carbonates. Furthermore, the range of fabrics between fluvial samples and location of the fluvial carbonates is relatively less variable compared to the perched tufa (Figs. 6A, 6D, 7B, 9C, 11). All samples found *in situ* fully or partially submerged in the spring display a distinct stromatolitic, cauliflower-like texture (Figs. 9A-C, 11). Similar fabrics have been previously observed in carbonates and they are typically associated with the presence of microbes (Gérard et al., 2018; Suchý et al., 2019; Pacton et al., 2015; Benson, 1994; Sanders et al., 2006; Chafetz & Folk, 1984). Diatoms were present in the laminated crust of one fluvial sample that was found partially submerged in the spring, but diatom presence in other fluvial samples could not be determined because their outer features were not mounted on thin section. It is possible that the smaller, rounded fossilized biota are cyanobacteria commonly associated with diatoms in freshwater settings (e.g., Saghaï et al., 2015; Gérard et al., 2018; Cantonati et al., 2012; Pacton et al., 2015), which would need to be confirmed with SEM analysis and microbiological examination. There were fewer distinct molds of diatom frustules found in the fluvial carbonate, implying that they have experienced less erosional and diagenetic events since deposition. There is no correlation between crystal size and biota presence and they appear laterally continuous in thin section (Fig. 9E-F). However, the least densely lithified areas/laminae are correlated with diatom presence, reinforcing the role of diatoms in creating porous fabrics in this setting (Boelts et al., 2020) and may contribute to the formation of the cauliflower-like fabric (see Multiscale Biosignature Analysis). Moreover, cauliflower-like fabrics have been observed to be produced in relatively calm, shallow-water settings (Benson, 1994; Pacton et al., 2015; Suchý et al., 2019; Gérard et al., 2018), which may explain why cauliflower-like fabric is absent from the perched tufa.

The sample collected adjacent to the fluvial carbonates further suggests that the depositional setting has shifted over time. However, it is unclear whether we found this sample in its true depositional environment or if it was transported some time ago. The well lithified, laminar internal structure corresponds more closely with the perched tufa rather than the fluvial carbonates. Its distinct banding also contains altering, stromatolitic laminae that contain calcified algae (Fig. 10), similar to the internal structures of the perched tufa. Although, the banding in this sample is relatively more laterally continuous suggesting it was deposited in less turbulent flow and contains fewer pores pointing to less erosional or diagenetic events. The laminae alternate between light-colored spar containing fossilized *Oocardium* and darker colored, porous micrite (Fig. 10). The micritic bands may contain diatoms but this would need to be confirmed using SEM analysis.

5.2.1 Seasonal Patterns

The internal structures of tufa are controlled by various local conditions related to topography and hydrology (Pedley, 1990) as well as the organisms that colonize its surface (Kano & Fuji, 2000). Internal banding was observed in both the perched and fluvial carbonates. The presence of annual or seasonal banding in cold-water carbonates can also offer a high-resolution paleoenvironmental record of short-term changes in climate (Matsuoka et al., 2001; Kano et al., 2004, 2003; Andrews & Brasier, 2005; Kano & Fuji, 2000; Brasier et al., 2010; Pedley & Rogerson, 2010). Like tree rings, the laminations typically show a regular rhythm of growth and their growth reflects seasonal patterns and changes in local environment and climate (Kano & Fuji, 2000; Arenas et al., 2014). The color and texture of each lamination reflects the conditions—or season—that it formed in (Kano & Fuji, 2000; Andrews & Brasier, 2005). For example, in Japan (Kano & Fuji, 2000) and Germany (Arp et al., 2001) lighter laminae were associated with higher water temperatures (warmer months) and darker laminae were associated with colder water temperatures (cooler months). The opposite patterns have been observed in other parts of the world—implying that depositional controls differ regionally (Viles & Pentecost, 2008; Pentecost & Spiro, 1990; Freytet and Plet, 1996; Janssen et al., 1999; Monty, 1976). Moreover, light and dark laminae can also be associated with seasonal changes in biota (Freytet & Plet, 1996; Viles & Pentecost, 2008; Pedley & Rogerson, 2010, 2010; Arp et al., 2001; Kano et al., 2003). The *Oocardium*-bearing laminations in samples from Henry Cowell State Park were likely formed during the summer, or warmer months of the year (see Significant Calcifying Biota). Since there is a lack of biota present in the banding of the fluvial tufas, stable oxygen isotope analysis should be carried out to see which texture and color corresponds to which season (see Future Work).

Texture—i.e., dense and porous—has also been observed to change seasonally in laminations (Arenas & Jones, 2017; Arenas et al., 2014; Viles & Pentecost, 2008; Arp et al., 2001; Kano et al., 2003; Andrews & Brasier, 2005; Matsuoka et al., 2001). However, there are chronological constraints to tufa laminations (Kano & Fuji, 2000; Andrews & Brasier, 2005). For instance, if a stream is not active throughout an entire year, tufa deposition will cease (Kano & Fuji, 2000). Furthermore, certain biota such as endolithic bacteria or the roots of plants can penetrate the tufa, thus obscuring the internal structures (Kano & Fuji, 2000; Arp et al., 2001). These factors should be considered when analyzing tufa laminations for paleoclimate information.

5.3 Significant Calcifying Biota

There are two common microphytes in the Santa Cruz region that are involved in the formation of tufa: *Oocardium stratum* and diatoms. *Oocardium* is a freshwater algae that is known to thrive in ambient-temperature, high-velocity spring waters and secretes extracellular polymeric substances (EPS), which induces calcite formation around its cell structure (Ibarra & Sanon, 2019; Sanders & Rott, 2009; Gradziński, 2010; Rott et al., 2010). In other tufa-depositing springs, the rate of *Oocardium* calcification has been observed to be more rapid than abiotic calcification by one to three orders of magnitude (Sanders & Rott, 2009). In samples collected from Santa Cruz, the presence of *Oocardium* can be seen at the meso (centimeters) scale in the form of distinct white/cream banding (Fig. 6A) as well as mm-scale dendritic shrubs (Fig. 6E) (Ibarra & Sanon, 2019). The presence of *Oocardium* in tufa settings can be indicative of seasonal deposition; in similar settings *Oocardium* is known to thrive during the warmer, "well-lit" months of the year (Sanders & Rott, 2009). Therefore, the *Oocardium*-bearing laminations in samples used in this study were likely formed during the warmer months of the year, while the darker, micritic laminations were formed during the colder months. This should be corroborated with stable isotope analysis, however.

The diatoms that have been identified prior to this study in thin section and coated grains (see Boelts et al., 2020) from Henry Cowell State Park primarily consist of two morphological groups: pennate (common) and centric (less common). The presence of diatoms in this setting signals that the water contains silica, which is needed for the diatoms to produce their frustules (Leng & Marshall, 2004; Viles & Pentecost, 2008). Unlike *Oocardium*, diatoms in similar freshwater tufa settings have been observed to be the most abundant during the winter months (Golubić et al., 2008; Arp et al., 2010; Sanders & Rott, 2009; Plee et al., 2008). Diatoms are also known to secrete extracellular polymeric substances (EPS), which contributes to the porosity of tufas in Henry Cowell State Park (Boelts et al., 2020), and have been commonly observed in micritic tufa in similar settings (Gradziński, 2010). However, diatom distribution in fluvial and perched samples is not always attributed to micritic banding (Fig. 9D-F). Diatoms may be present within darker, micritic laminae but this would need to be confirmed with SEM analysis. Until then, their unequivocal biosignatures at the micro and meso scales cannot be determined. Moreover, their association with other algal flora and distribution throughout the carbonate stream in Henry Cowell State Park remains unknown.

5.4 Astrobiological Implications

Fluvial tufa settings are key targets in the search for potential biosignatures on other planets like Mars due to their rapid lithifying nature, which can preserve aquatic microorganisms. The lack of tectonic activity on Mars and the slower weathering rates compared to Earth, suggests Mars may serve as a window into early Earth environments (McMahon et al., 2018; Cady et al., 2003; Farmer & Des Marais 1999; Michalski et al. 2017; Ramirez & Craddock, 2018; Wordsworth, 2016; Farley et al., 2020). Networks of valleys and sedimentary rocks dating back to the Noachian and Hesperian Periods (roughly 4-3.6 billion years ago) allude to Mars as a much more habitable planet with a relatively high abundance of liquid water at its surface (McMahon et al., 2018; Farmer & Des Marais, 1999; Michalski et al., 2017; Horgan et al., 2020; Cabrol & Grin, 1999; Ramirez & Craddock, 2018; Niles et al., 2013; Williford et al., 2018; Wordsworth, 2016). Furthermore, orbital data has shown significant geomorphological features that are typically formed by liquid water such as fluvial valleys, paleolake deposits, meandering and braided channels, alluvial fans and deltas—some of which have been interpreted as opening onto the shoreline of an ocean (McMahon et al., 2018, Cabrol & Grin, 1999; Fassett & Head, 2008; Goudge et al., 2016; Grant et al., 2008; Grotzinger, Gupta, et al., 2015; Malin & Edgett, 2003; Metz et al., 2009; Moore & Howard, 2005, Horgan et al., 2020; Wordsworth, 2016; Farley et al., 2020). These environments could have hosted microbial life and suggests that the planet also had a denser atmosphere (McMahon et al., 2018; Ramirez & Craddock, 2018; Niles et al., 2013; Michalski et al., 2017; Horgan et al., 2020; Grotzinger et al., 2015).

The twin Viking landers in 1976 marks the first NASA mission that prioritized searching for life on other planets (Williford et al., 2018). The missions that followed began to evolve from seeking evidence of modern life on Mars, and rather toward looking for traces of ancient life (Williford et al., 2018). Evidence pointing to early Mars containing surface water, a magnetic field, and an atmosphere—being more Earth-like—stirred up excitement about the implications of past habitable environments and planetary evolution (Williford et al., 2018). Thus, the scientific community has shifted its focus toward the exploration of ancient environments that have the potential of yielding biosignatures (Williford et al., 2018). The missions to Mars that have followed the twin Viking rovers have confirmed the presence of carbonates on its surface (Horgan et al., 2020, Ehlmann et al., 2008; Morris et al., 2010; Michalski & Niles, 2010). NASA's Perseverance rover will investigate carbonates in Jezero Crater, which was once a fluvio-lacustrine depositional setting that may have been conducive to creating and preserving tufa-like deposits (Williford et al., 2018; Horgan et al., 2020; Farley et al., 2020). Moreover, the rover will seek to collect samples for possible Earth return (Williford et al., 2018; Farley et al., 2020).

5.4.1 Multiscale Biosignature Analysis

Biosignatures are signs of life that are preserved in the rock record as morphological microfossils, macroscopic sedimentary structures, or chemofossils (Potter-McIntyre et al. 2017; Cady and Noffke, 2009; Cady et al., 2003). Biosignature interpretation is not always straight-forward, the preservation of biosignatures is often affected by events (e.g., weathering) that occur after deposition as well as the stability of primary minerals (Hays et al., 2017; Cady et al., 2003). Characterizing multiple types of biosignatures at macro-scales has been deemed a priority for the Mars 2020 mission (Hays et al., 2017). Considering the limitations of our own knowledge of Earth's early life in the rock record (e.g., Brasier et al., 2002; Schopf, 1993), it is unlikely the

Perseverance rover will be able to give substantial evidence to show the planet was once inhabited (Farley et al., 2020). Therefore, we are more concerned with identifying samples that have the greatest biosignature preservation potential for Earth sample return (Williford et al., 2018; Farley et al., 2020). Furthermore, the lack of evidence of life on Mars would also be a scientifically novel result (Farley et al., 2020). Such a result would indicate that some environments that may be considered habitable by Earth standards are not always inhabited—thus contributing to our model of habitability beyond our own planet (Farley et al., 2020).

Stromatolites have been deemed particularly significant for biosignature investigations on Mars as well as paleoclimate studies (Shiraishi et al., 2010; Gammeriello et al., 2014; Petryshyn et al., 2012; Andrews & Brasier, 2005; Arenas & Jones, 2017; Capezzuoli et al., 2014; Eymard et al., 2020). Ancient stromatolites contain the earliest record of life on Earth (Hofmann et al., 1999; Allwood et al., 2009; Awramik & Sprinkle, 1999) and are defined as "an attached, laminated, lithified sedimentary growth structure, accretionary away from a point or limited surface of initiation" (Semikhatov et al., 1979). They typically contain successive millimeter- or micrometer-scale laminae that accrete upward and can be flat, domal, coniform, columnar, or branching columnar in shape (Cady et al., 2003; Bosak et al., 2013; Riding, 2000). Their production is thought to be aided by algae via biologically-induced calcite precipitation or trapping and binding of sediment (Gammeriello et al., 2014; Bosak et al., 2013; Dupraz et al., 2009; Riding, 2000). However, the extent to which biological inputs influence the formation of stromatolites, and therefore their unequivocal biosignatures, remains unclear (Ibarra & Corsetti, 2016; Buick et al., 1981; Lowe, 1994; Grotzinger & Knoll, 1999; Lindsay et al., 2003; Andrews & Brasier, 2005; Riding, 2000).

Given the evidence of past fluvial settings on Mars (McMahon et al., 2018, Cabrol & Grin, 1999; Fassett & Head, 2008; Goudge et al., 2016; Grant et al., 2008; Grotzinger, Gupta, et al., 2015; Malin & Edgett, 2003; Metz et al., 2009; Moore & Howard, 2005, Horgan et al., 2020; Wordsworth, 2016; Farley et al., 2020), the fluvial carbonates from Henry Cowell State Park may serve as an appropriate proxy. The domal, cauliflower-like fabric displayed in the fluvial tufas (Figs. 9A-C, 11) has a relatively high biosignature potential, as observed by the literature (Gérard et al., 2018; Suchý et al., 2019; Pacton et al., 2015; Benson, 1994; Sanders et al., 2006). Moreover, this fabric is easily distinguishable at a macro-scale that can be identified by current rover technology. In cross-section and thin section, these domes display a stromatolitic fabric—each individual bump is representative of one micro-scale domed stromatolite (Figs. 9C-D, 11). The micro-scale domes are seemingly biotically controlled, however the larger scale, meso-scale bulges and internal fabrics are ambiguous in origin. The amount of variability in the morphology of fabrics at this scale implies controls that are abiotic (e.g., water flow, water chemistry, clastic material).

At the micro scale, we noted distinct banding and the presence of diatoms (Fig. 9D-F) indicating seasonal patterns as well as biotic controls. Laterally continuous diatom presence points to laminae as a calcified microbial mat. This suggests that the EPS from the diatoms would have contributed to tufa growth. The alterations between dense laminae and non-densely lithified laminae containing diatoms suggests that seasonal, abiotic factors are at play as well. This implies that the more porous bands formed during seasons that favor diatom presence and the dense bands formed during a subsequent season when diatoms are not present. However, this should be further investigated using stable isotope analysis of carbonate oxygen and carbon to identity potential seasonal trends. The outer crust of the sample contains a distinct domal shape that alludes to an up-direction. On the other hand, the more internal banding is noticeably flatter and does not contain a clear up direction. It is possible the smaller, mm-sized, mounds are a consequence of microbial growth, which is further supported by the presence of biota in the outer layers and no known fossils in the inner features. This would need to be further investigated through SEM analysis, which would reveal potential microbial traces in the internal, older textures.

Our observations of the tufa fabrics from Henry Cowell State Park enforces that the role of microorganisms in tufa formation is ambiguous, but not passive. Overall, our investigation supports the idea that as we scale up the controls of the tufa features, they begin to transition from biotic to abiotic, local to nonlocal (see Ibarra & Corsetti, 2016) (Table 1). Given our evidence of some extent of biotic input and evidence from literature of similar cauliflower-like fabrics associated with microbes, this fabric has a high biosignature potential. Regardless of whether laminations contain fossilized microbes, their correlation to seasonality is highly significant. Therefore, this macro to micro-scale texture should be considered for their biosignature potential/Earth sample return if found on Mars. Given the relationship between diatom presence and porous fabrics in tufas from similar settings (Arp et al., 2001; Gradziński, 2010), it would be advised that SEM analysis is considered in future investigations. It should also be noted that diatoms were not abundant on Earth until the late Cretaceous (Riding, 2000) and we would therefore not expect to find diatom-induced morphologies in Mars' rock record. However, amorphous biofilms such as EPS produced by diatoms and other algae and bacteria would be important contributors to fabric alteration.

6. Conclusions

The spring-associated tufas in the Santa Cruz, CA region are a valuable addition to the Quaternary paleohydroclimate record of the region. Moreover, they serve as promising proxies to inform the search of life on Mars. The ages of the ancient tufa from Pogonip Park and Henry Cowell State Park—from ^{14}C and IRSL analyses—corroborate other regional records of paleoclimate and support wetter conditions (i.e. pluvials) during the Pleistocene-Holocene transition. The differences between the perched and fluvial carbonates point to two different depositional settings; the perched carbonates likely formed in a wetter climate and the fluvial carbonates formed in a dryer, more modern-day setting. IRSL dates reveal the tufa cascade in Pogonip Park was active from ~10.4 to 14 ka, which is slightly older than when the perched tufa in Henry Cowell State Park was active (~6 to 8 cy BP). These ages agree with the timing of what other regional proxies reveal to be a colder, wetter climate. Moreover, the presence of *Oocardium* in the inactive tufa indicates the depositional setting experienced higher water levels than today. ^{14}C analysis of charcoal from the fluvial carbonates show that they formed relatively more recently (~850 years BP) and likely under present-day conditions. Seasonal patterns are evident in both ancient and modern samples from Henry Cowell, which should be investigated further using stable isotope analysis. The cauliflower-like external fabric of the fluvial carbonates has significant biosignature potential and its micro-scale features are likely formed, in-part, biotically. This should, however, be further investigated using SEM analysis. Furthermore, the larger-scale features were likely the consequence of abiotic inputs. Should this fabric be identified on Mars, it should be considered for Earth sample return.

7. Future Work

Due to the COVID-19 pandemic, several analyses were left out of this study but should be considered for future work. First, stable isotope analysis of carbonate would be useful for determining the depositional processes that influenced tufa formation (Swart, 2015) and present a regional paleoclimate record (Andrews, 2006). Specifically, oxygen isotope values reveal the temperature of the water in which each lamination in a tufa formed (Andrews and Brasier, 2005). Carbon isotope values in carbonates reflect local carbon contributions (Swart, 2015). Next, scanning electron microscopy (SEM) would reveal if and what microbe morphologies are present in samples that could not be determined with light microscopy. Lastly, the pollen that has been collected from the cores would be a valuable proxy for corroborating the region's existing pollen record as well as the broader paleoclimate record. Moreover, there is currently no pollen record from Santa Cruz, CA, adding to its scientific value.

References

University of California, Santa Cruz Long-Range Development Plan 2005-2020 Draft, 2005, https://lrdp.ucsc.edu/Draft2005EIR/2005deir-4.6-geology.pdf.

Ringtail Creek, http://us.geoview.info/ringtail_creek,42854550w (accessed February 2020).

Adam, D.P., Sims, J.D., and Throckmorton, C.K., 1981, 130 ,000-yr continuous pollen record from Clear Lake, Lake County, California: Geology, v. 9, p. 373–377.

Aitken, M.J., 1998, Introduction to optical dating: Quaternary sediments by the use of photon-stimulated luminescence: Oxford University Press.

Allwood, A.C., Grotzinger, J.P., Knoll, A.H., Burch, I.W., Anderson, M.S., Coleman, M.L., and Kanik, I., 2009, Controls on development and diversity of Early Archean stromatolites: Proceedings of the National Academy of Sciences of the United States of America, v. 106, p. 9548–9555, doi:10.1073/pnas.0903323106.

Anderson, R.S., and Menking, K.M., 1994, The Quaternary marine terraces of Santa Cruz, California: evidence for coseismic uplift on two faults: Geological Society of America Bulletin, v. 106, p. 649–664, doi:10.1130/0016-7606(1994)106<0649:TQMTOS>2.3.CO;2.

Andrews, J.E., 2006, Palaeoclimatic records from stable isotopes in riverine tufas: Synthesis and review: Earth-Science Reviews, v. 75, p. 85–104, doi:10.1016/j.earscirev.2005.08.002.

Andrews, J.E., and Brasier, A.T., 2005, Seasonal records of climatic change in annually laminated tufas: Short review and future prospects: Journal of Quaternary Science, v. 20, p. 411–421, doi:10.1002/jqs.942.

Andrews, J.E., Pedley, M., and Dennis, P.F., 2000, Palaeoenvironmental records in Holocene Spanish tufas: A stable isotope approach in search of reliable climatic archives: Sedimentology, v. 47, p. 961–978, doi:10.1046/j.1365-3091.2000.00333.x.

Arenas, C., and Jones, B., 2017, Temporal and environmental significance of microbial lamination: Insights from Recent fluvial stromatolites in the River Piedra, Spain: Sedimentology, v. 64, p. 1597–1629, doi:10.1111/ijlh.12426.

Arenas, C., Vázquez-Urbez, M., Auqué, L., Sancho, C., Osácar, C., and Pardo, G., 2014, Intrinsic and extrinsic controls of spatial and temporal variations in modern fluvial tufa sedimentation: A thirteen-year record from a semi-arid environment: Sedimentology, v. 61, p. 90–132, doi:10.1111/sed.12045.

Arenas, C., Vázquez-Urbez, M., Pardo, G., and Sancho, C., 2014, Sedimentology and depositional architecture of tufas deposited in stepped fluvial systems of changing slope: Lessons from the quaternary añamaza valley (Iberian Range, Spain): Sedimentology, v. 61, p. 133–171, doi:10.1111/sed.12053.

Arp, G., Wedemeyer, N., and Reitner, J., 2001, Fluvial tufa formation in a hard-water creek (Deinschwanger Bach, Franconian Alb, Germany): Facies, v. 37, p. 1–22, doi:10.1007/bf02668163.

Arp, G. et al., 2010, Tufa-forming biofilms of German karstwater streams: Microorganisms, exopolymers, hydrochemistry and calcification: Geological Society Special Publication, v. 336, p. 83–118, doi:10.1144/SP336.6.

Awramik, S.M., and Sprinkle, J., 1999, Proterozoic stromatolites: The first marine evolutionary biota: Historical Biology, v. 13, p. 241–253.

Benson, L., 1994, Carbonate deposition, Pyramid Lake subbasin, Nevada: 1. Sequence of formation and elevational distribution of carbonate deposits (Tufas): Palaeogeography, Palaeoclimatology, Palaeoecology, v. 109, p. 55–87, doi:10.1016/0031-0182(94)90118-X.

Beverly, E.J., Driese, S.G., Peppe, D.J., Johnson, C.R., Michel, L.A., Faith, J.T., Tryon, C.A., and Sharp, W.D., 2015, Recurrent spring-fed rivers in a Middle to Late Pleistocene semi-arid grassland: Implications for environments of early humans in the Lake Victoria Basin, Kenya: Sedimentology, v. 62, p. 1611–1635, doi:10.1111/sed.12199.

Boelts, H., Ibarra, Y., and Hayzelden, C., 2020, Investigating the Influence of Diatoms on the Textures of Coated Grains From a Carbonate Spring in Northern California: Journal of Sedimentary Research, v. 90, p. 1601–1613, doi:10.1130/abs/2020am-359415.

Bosak, T., Knoll, A.H., and Petroff, A.P., 2013, The meaning of stromatolites: Annual Review of Earth and Planetary Sciences, v. 41, p. 21–44, doi:10.1146/annurev-earth-042711-105327.

Brabb, E.E., 1983, Studies in Tertiary stratigraphy of the California Coast Ranges.: US Geological Survey Professional Paper, v. 1213.

Bradley, W.C., 1957, ORIGIN OF MARINE-TERRACE DEPOSITS IN THE SANTA CRUZ AREA, CALIFORNIA: Bulletin of the Geological Society of America, v. 68, p. 421–444, doi:10.1017/CBO9781107415324.004.

Brasier, A.T., Andrews, J.E., Marca-Bell, A.D., and Dennis, P.F., 2010, Depositional continuity of seasonally laminated tufas: Implications for δ18O based palaeotemperatures: Global and Planetary Change, v. 71, p. 160–167, doi:10.1016/j.gloplacha.2009.03.022.

Brasier, M.D., Green, O.R., Jephcoat, A.P., Kleppe, A.K., Kranendonk, M.J. Van, Lindsay, J.F., Steele, A., and Grassineau, N. V, 2002, Questioning the evidence for Earth's oldest fossils: Nature, v. 416, p. 76–81.

Buick, R., Dunlop, J.S., and Groves, D.I., 1981, Stromatolite recognition in ancient rocks: An appraisal of irregularly laminated structures in an early Archaean chert-barite unit from north pole, Western Australia: Alcheringa, v. 5, p. 161–181, doi:10.1080/03115518108566999.

Cabrol, N.A., and Grin, E.A., 1999, Distribution, Classification, and Ages of Martian Impact Crater Lakes: Icarus, v. 142, p. 160–172, doi:10.1006/icar.1999.6191.

Cady, S.L., Farmer, J.D., Grotzinger, J.P., Schopf, J.W., and Steele, A., 2003, Morphological biosignatures and the search for life on mars: Astrobiology, v. 3, p. 351–368, doi:10.1089/153110703769016442.

Cady, S.L., and Noffke, N., 2009, Geobiology: Evidence for early life on earth and the search for life on other planets: GSA Today, v. 19, p. 4–10, doi:10.1130/GSATG62A.1.

California State Parks, 2011, Henry Cowell Redwoods State Park:

Cantonati, M., Angeli, N., Bertuzzi, E., Spitale, D., and Lange-Bertalot, H., 2012, Diatoms in springs of the Alps: Spring types, environmental determinants, and substratum: Freshwater Science, v. 31, p. 499–524, doi:10.1899/11-065.1.

Capezzuoli, E., Gandin, A., and Pedley, M., 2014, Decoding tufa and travertine (freshwater carbonates) in the sedimentary record: The state of the art: Sedimentology, v. 61, p. 1–21, doi:10.1111/sed.12075.

Chafetz, H.S., and Folk, R.L., 1984, Travertines: Depositional Morphology and the Bacterially Constructed Constituents: SEPM Journal of Sedimentary Research, v. 54, p. 289–316.

Cook, E.., Seager, R., Heim, R.R., Vose, R.S., Herweijer, C., and Woodhouse, C., 2010, Megadroughts in North America: placing IPCC projections of hydroclimate change in a long-term paleoclimate context: Journal of Quaternary Science, v. 25, p. 48-61.

Cremaschi, M., Zerboni, A., Spötl, C., and Felletti, F., 2010, The calcareous tufa in the Tadrart Acacus Mt. (SW Fezzan, Libya). An early Holocene palaeoclimate archive in the central Sahara: Palaeogeography, Palaeoclimatology, Palaeoecology, v. 287, p. 81–94, doi:10.1016/j.palaeo.2010.01.019.

Desouky, H. El, Soete, J., Claes, H., Özkul, M., Vanhaecke, F., and Swennen, R., 2015, Novel applications of fluid inclusions and isotope geochemistry in unravelling the genesis of fossil travertine systems: Sedimentology, v. 62, p. 27–56, doi:10.1111/sed.12137.

Domínguez-Villar, D., Vázquez-Navarro, J.A., Cheng, H., and Edwards, R.L., 2011, Freshwater tufa record from Spain supports evidence for the past interglacial being wetter than the Holocene in the Mediterranean region: Global and Planetary Change, v. 77, p. 129–141, doi:10.1016/j.gloplacha.2011.04.006.

Dupraz, C., Reid, R.P., Braissant, O., Decho, A.W., Norman, R.S., and Visscher, P.T., 2009, Processes of carbonate precipitation in modern microbial mats: Earth-Science Reviews, v. 96, p. 141–162, doi:10.1016/j.earscirev.2008.10.005.

Ehlmann, B.L., Mustard, J.F., Murchie, S.L., Poulet, F., Bishop, J.L., Roach, L.H., Roush, T.L., Swayze, G.A., and Wray, J.J., 2008, Orbital Identification of Carbonate-Bearing Rocks on Mars: Science, v. 322, p. 1828–1832.

Eymard, I., del Pilar Alvarez, M., Bilmes, A., Vasconcelos, C., and Ariztegui, D., 2020, Tracking Organomineralization Processes from Living Microbial Mats to Fossil Microbialites: Minerals, v. 10, p. 1–20.

Farley, K.A. et al., 2020, Mars 2020 Mission Overview: Space Science Reviews, v. 216, doi:10.1007/s11214-020-00762-y.

Farmer, J.D., and Des Marais, D.J., 1999, Exploring for a record of ancient Martian life: Journal of Geophysical Research E: Planets, v. 104, p. 26977–26995, doi:10.1029/1998JE000540.

Fassett, C.I., and Head, J.W., 2008, Valley network-fed, open-basin lakes on Mars: Distribution and implications for Noachian surface and subsurface hydrology: Icarus, v. 198, p. 37–56, doi:10.1016/j.icarus.2008.06.016.

Ford, T.D., and Pedley, H.M., 1996, A review of tufa and travertine deposits of the world: Earth-Science Reviews, v. 41, p. 117–175, doi:10.1016/s0012-8252(96)00030-x.

Freytet, P., and Plet, A., 1996, Modern freshwater microbial carbonates: The Phormidium stromatolites (tufa-travertine) of Southeastern Burgundy (Paris Basin, France): Facies, p. 219–237, doi:10.1007/bf02546166.

Gammeriello, R., Ibarra, Y., Pietsch, C., and Petryshyn, V., 2014, Using stromatolites to constrain temperatures during times of biotic crisis, and comparing them to a mineralogically derived climate model of Mars:, http://pdsmgmt.gsfc.nasa.gov/education/csi/current_cohort/GammarielloFINAL.pdf%0Apapers3://publication/uuid/4FED1ECC-DEA3-4155-83D6-E84A792F5DD3.

Gardner, J. V, Park, M., Heusser, L.E., Quinterno, P.J., Stone, S.M., and Barron, J.A., 1988, Clear Lake record vs. the adjacent marine record; A correlation of their past 20,000 years of paleoclimatic and paleooceanographic responses: Geologic Society of America, p. 171–182.

Gérard, E. et al., 2018, Key role of Alphaproteobacteria and Cyanobacteria in the formation of stromatolites of Lake Dziani Dzaha (Mayotte, Western Indian Ocean): Frontiers in Microbiology, v. 9, p. 1–20, doi:10.3389/fmicb.2018.00796.

Gérard, E., Ménez, B., Couradeau, E., Moreira, D., Benzerara, K., Tavera, R., and López-García, P., 2013, Specific carbonate-microbe interactions in the modern microbialites of Lake Alchichica (Mexico): ISME Journal, v. 7, p. 1997–2009, doi:10.1038/ismej.2013.81.

Golubić, S., Violante, C., Plenković-Moraj, A., and Gragasović, T., 2008, Travertines and calcareous tufa deposits: An insight into diagenesis: Geologia Croatica, v. 61, p. 363–378, doi:10.4154/GC.2008.28.

Goudge, T.A., Fassett, C.I., Head, J.W., Mustard, J.F., and Aureli, K.L., 2016, Insights into surface runoff on early Mars from paleolake basin morphology and stratigraphy: Geology, v. 44, p. 419–422, doi:10.1130/G37734.1.

Gradziński, M., 2010, Factors controlling growth of modern tufa: Results of a field experiment: Geological Society Special Publication, v. 336, p. 143–191, doi:10.1144/SP336.8.

Grant, J.A., Irwin, R.P., Grotzinger, J.P., Milliken, R.E., Tornabene, L.L., McEwen, A.S., Weitz, C.M., Squyres, S.W., Glotch, T.D., and Thomson, B.J., 2008, HiRISE imaging of impact megabreccia and sub-meter aqueous strata in Holden Crater, Mars: Geology, v. 36, p. 195–198, doi:10.1130/G24340A.1.

Grotzinger, J.P. et al., 2015, Deposition, exhumation, and paleoclimate of an ancient lake deposit, Gale crater, Mars: Science, v. 350, doi:10.1126/science.aac7575.

Grotzinger, J.R., and Knoll, A.H., 1999, Stromatolites in Precambrian carbonates: Evolutionary mileposts or environmental dipsticks? Annual Review of Earth and Planetary Sciences, v. 27, p. 313–358, doi:10.1146/annurev.earth.27.1.313.

Halevy, I., Fischer, W.W., and Eiler, J.M., 2011, Carbonates in the Martian meteorite Allan Hills 84001 formed at 18 ± 4 °C in a near-surface aqueous environment: Proceedings of the National Academy of Sciences of the United States of America, v. 108, p. 16895–16899, doi:10.1073/pnas.1109444108.

Hays, L.E., Graham, H. V., Des Marais, D.J., Hausrath, E.M., Horgan, B., McCollom, T.M., Parenteau, M.N., Potter-McIntyre, S.L., Williams, A.J., and Lynch, K.L., 2017, Biosignature Preservation and Detection in Mars Analog Environments: Astrobiology, v. 17, p. 363–400, doi:10.1089/ast.2016.1627.

Heusser, L.E., and Shackleton, N.J., 1979, Direct Marine-Continental Correlation: 150,000-Year Oxygen Isotope-Pollen Record from the North Pacific: Science, v. 204, p. 837–839.

Hofmann, H.J., Grey, K., Hickman, A.H., and Thorpe, R.I., 1999, Origin of 3.45 Ga coniform stromatolites in Warrawoona Group, Western Australia: Bulletin of the Geological Society of America, v. 111, p. 1256–1262, doi:10.1130/0016-7606(1999)111<1256:OOGCSI>2.3.CO;2.

Horgan, B.H.N., Anderson, R.B., Dromart, G., Amador, E.S., and Rice, M.S., 2020, The mineral diversity of Jezero crater: Evidence for possible lacustrine carbonates on Mars: Icarus, v. 339, p. 113526, doi:10.1016/J.ICARUS.2019.113526.

Huntley, D.J., Lamothe, M., 2001, Ubiquity of anomalous fading in K-feldspars and the measurement and correction for it in optical dating: Canadian Journal of Earth Sciences, v. 38, p. 1093-1106, doi:10.1139/cjes-38-7-1093.

Ibarra, Y., and Corsetti, F.A., 2016, Lateral comparative investigation of stromatolites: Astrobiological implications and assessment of scales of control: Astrobiology, v. 16, p. 271–281, doi:10.1089/ast.2015.1388.

Ibarra, Y., Corsetti, F.A., Feakins, S.J., Rhodes, E.J., and Kirby, M.E., 2015, Fluvial tufa evidence of Late Pleistocene wet intervals from Santa Barbara, California, U.S.A.: Palaeogeography, Palaeoclimatology, Palaeoecology, v. 422, p. 36–45, doi:10.1016/J.PALAEO.2015.01.012.

Ibarra, Y., and Sanon, S., 2019, A freshwater analog for the production of Epiphyton-like microfossils: Geobiology, v. 17, p. 510–522, doi:10.1111/gbi.12341.

Janssen, A., Swennen, R., Podoor, N., and Keppens, E., 1999, Biological and diagenetic influence in Recent and fossil tufa deposits from Belgium: Sedimentary Geology, v. 126, p. 75–95, doi:10.1016/S0037-0738(99)00033-0.

Kano, A., and Fujii, H., 2000, Origin of the gross morphology and internal texture of tufas of Shirokawa Town, Ehime Prefecture, southwest Japan: Journal of the Geological Society of Japan, v. 106, p. 397–412, http://www.mendeley.com/research/geology-volcanic-history-eruptive-style-yakedake-volcano-group-central-japan/.

Kano, A., Kawai, T., Matsuoka, J., and Ihara, T., 2004, High-resolution records of rainfall events from clay bands in tufa: Geology, v. 32, p. 793–796, doi:10.1130/G20736.1.

Kano, A., Matsuoka, J., Kojo, T., and Fujii, H., 2003, Origin of annual laminations in tufa deposits, southwest Japan: Palaeogeography, Palaeoclimatology, Palaeoecology, v. 191, p. 243–262, doi:10.1016/0031-0182(02)00717-4.

Lee, E.S. (University of C.S.C., 1992, THE POGONIP DECONSTRUCTED: The geologic and human contributions to the landscape: Universitgy of California, Santa Cruz, 1–37 p.

Leng, M.J., and Marshall, J.D., 2004, Palaeoclimate interpretation of stable isotope data from lake sediment archives: Quaternary Science Reviews, v. 23, p. 811–831, doi:10.1016/j.quascirev.2003.06.012.

Lindsay, J.F., Brasier, M.D., McLoughlin, N., Green, O.R., Fogel, M., McNamara, K.M., Steele, A., and Mertzman, S.A., 2003, Abiotic Earth -- Establishing a Baseline for Earliest Life, Data from the Archean of Western Australia: 34th Annual Lunar and Planetary Science Conference, v. XXXIV, p. 1137.pdf, http://adsabs.harvard.edu/abs/2003LPI....34.1137L.

Lowe, D.R., 1994, Abiological origin of described stromatolites older than 3.2 Ga: reply.: Geology, v. 23, p. 191–192.

Lyle, M., Heusser, L., Herbert, T., Mix, A., and Barron, J., 2001, Interglacial theme and variations: 500 k.y. of orbital forcing and associated responses from the terrestrial and marine biosphere, U.S. Pacific Northwest: Geology, v. 29, p. 1115–1118, doi:10.1130/0091-7613(2001)029<1115:ITAVKY>2.0.CO;2.

Lyle, M., Heusser, L., Ravelo, C., Andreasen, D., Olivarez Lyle, A., and Diffenbaugh, N., 2010, Pleistocene water cycle and eastern boundary current processes along the California continental margin: Paleoceanography, v. 25, p. 1–19, doi:10.1029/2009PA001836.

Lyle, M., Heusser, L., Ravelo, C., Yamamoto, M., Barron, J., Diffenbaugh, N.S., Herbert, T., and Andreasen, D., 2012, Out of the tropics: The pacific, great basin lakes, and late Pleistocene water cycle in the western United States: Science, v. 337, p. 1629–1633, doi:10.1126/science.1218390.

Malin, M.C., and Edgett, K.S., 2003, Conference on Early Mars: Science, v. 302, p. 1931–1934, doi:10.1126/science.1090544.

Martín-Algarra, A., Martín-Martín, M., Andreo, B., Julià, R., and González-Gómez, C., 2003, Sedimentary patterns in perched spring travertines near Granada (Spain) as indicators of the paleohydrological and paleoclimatological evolution of a karst massif: Sedimentary Geology, v. 161, p. 217–228, doi:10.1016/S0037-0738(03)00115-5.

Matsuoka, J., Kano, A., Oba, T., Watanabe, T., Sakai, S., and Seto, K., 2001, Seasonal variation of stable isotopic compositions recorded in a laminated tufa, SW Japan: Earth and Planetary Science Letters, v. 192, p. 31–44, doi:10.1016/S0012-821X(01)00435-6.

McMahon, S., Bosak, T., Grotzinger, J.P., Milliken, R.E., Summons, R.E., Daye, M., Newman, S.A., Fraeman, A., Williford, K.H., and Briggs, D.E.G., 2018, A Field Guide to Finding Fossils on Mars: Journal of Geophysical Research: Planets, v. 123, p. 1012–1040, doi:10.1029/2017JE005478.

Merz-Preiß, M., and Riding, R., 1999, Cyanobacterial tufa calcification in two freshwater streams: ambient environment, chemical thresholds and biological processes: Sedimentary Geology, v. 126, p. 103–124, doi:10.1016/S0037-0738(99)00035-4.

Metz, J.M., Grotzinger, J.P., Mohrig, D., Milliken, R., Prather, B., Pirmez, C., McEwen, A.S., and Weitz, C.M., 2009, Sublacustrine depositional fans in southwest Melas Chasma: Journal of Geophysical Research E: Planets, v. 114, p. 1–17, doi:10.1029/2009JE003365.

Michalski, J.R., and Niles, P.B., 2010, Deep crustal carbonate rocks exposed by meteor impact on Mars: Nature Geoscience, v. 3, p. 751–755, doi:10.1038/ngeo971.

Michalski, J.R., Onstott, T.C., Mojzsis, S.J., Mustard, J., Chan, Q.H.S., Niles, P.B., and Johnson, S.S., 2017, The Martian subsurface as a potential window into the origin of life: Nature Geoscience, v. 11, p. 21–26, doi:10.1038/s41561-017-0015-2.

Moore, J.M., and Howard, A.D., 2005, Large alluvial fans on Mars: Journal of Geophysical Research E: Planets, v. 110, p. 1–24, doi:10.1029/2004JE002352.

Morris, R. V. et al., 2010, Identification of carbonate-rich outcrops on Mars by the spirit rover: Science, v. 329, p. 421–424, doi:10.1126/science.1189667.

Niles, P.B., Catling, D.C., Berger, G., Chassefière, E., Ehlmann, B.L., Michalski, J.R., Morris, R., Ruff, S.W., and Sutter, B., 2013, Geochemistry of carbonates on Mars: Implications for climate history and nature of aqueous environments: Space Science Reviews, v. 174, p. 301–328, doi:10.1007/s11214-012-9940-y.

Oster, J.L., Montañez, I.P., Sharp, W.D., and Cooper, K.M., 2009, Late Pleistocene California droughts during deglaciation and Arctic warming: Earth and Planetary Science Letters, v. 288, p. 434–443, doi:10.1016/j.epsl.2009.10.003.

Oster, J.L., Sharp, W., Covey, A., Gibson, J., Rogers, B., and Mix, H., 2017, Climate responses to the 8.2 ka event in coastal California: Scientific Reports, v. 7, p. 1-9, doi:10.1038/s41598-017-04215-5.

Özkul, M., Kele, S., Gökgöz, A., Shen, C.C., Jones, B., Baykara, M.O., Fórizs, I., Németh, T., Chang, Y.W., and Alçiçek, M.C., 2013, Comparison of the Quaternary travertine sites in the Denizli extensional basin based on their depositional and geochemical data: Sedimentary Geology, v. 294, p. 179–204, doi:10.1016/j.sedgeo.2013.05.018.

Pacton, M., Hunger, G., Martinuzzi, V., Cusminsky, G., Burdin, B., Barmettler, K., Vasconcelos, C., and Ariztegui, D., 2015, Organomineralization processes in freshwater stromatolites: a living example from eastern Patagonia: The Depositional Record, v. 1, p. 130–146, doi:10.1002/dep2.7.

Pedley, H.M., 1990, Classification and environmental models of cool freshwater tufas: Sedimentary Geology, v. 68, p. 143–154, doi:10.1016/0037-0738(90)90124-C.

Pedley, H.M., and Rogerson, M., 2010, In vitro investigations of the impact of different temperature and flow velocity conditions on tufa microfabric: Geological Society Special Publication, v. 336, p. 193–210, doi:10.1144/SP336.9.

Pedley, H.M., and Rogerson, M., 2010, Introduction to tufas and speleothems: Geological Society Special Publication, v. 336, p. 1–5, doi:10.1144/SP336.1.

Pedley, M., 2009, Tufas and travertines of the Mediterranean region: A testing ground for freshwater carbonate concepts and developments: Sedimentology, v. 56, p. 221–246, doi:10.1111/j.1365-3091.2008.01012.x.

Pedley, M., González Martín, J.A., Ordónez Delgado, S., and García Del Cura, M.Á., 2003, Sedimentology of quaternary perched springline and paludal tufas: Criteria for recognition, with examples from Guadalajara Province, Spain: Sedimentology, v. 50, p. 23–44, doi:10.1046/j.1365-3091.2003.00502.x.

Pellicer, X.M., Linares, R., Gutiérrez, F., Comas, X., Roqué, C., Carbonel, D., Zarroca, M., and Rodríguez, J.A.P., 2014, Morpho-stratigraphic characterization of a tufa mound complex in the spanish pyrenees using ground penetrating radar and trenching, implications for studies in mars: Earth and Planetary Science Letters, v. 388, p. 197–210, doi:10.1016/j.epsl.2013.11.052.

Pentecost, A., and Spiro, B., 1990, Stable carbon and oxygen isotope composition of calcites associated with modern freshwater cyanobacteria and algae: Geomicrobiology Journal, v. 8, p. 17–26, doi:10.1080/01490459009377875.

Petryshyn, V.A., Corsetti, F.A., Berelson, W.M., Beaumont, W., and Lund, S.P., 2012, Stromatolite lamination frequency, Walker Lake, Nevada: Implications for stromatolites as biosignatures: Geology, v. 40, p. 499–502, doi:10.1130/G32675.1.

Plee, K., Ariztegui, D., Martini, R., and Davaud, E., 2008, Unravelling the microbial role in ooid formation - Results of an in situ experiment in modern freshwater Lake Geneva in Switzerland: Geobiology, v. 6, p. 341–350, doi:10.1111/j.1472-4669.2007.00140.x.

Potter-McIntyre, S.L., Williams, J., Phillips-Lander, C., and O'Connell, L., 2017, Taphonomy of Microbial Biosignatures in Spring Deposits: A Comparison of Modern, Quaternary, and Jurassic Examples: Astrobiology, v. 17, p. 216–230, doi:10.1089/ast.2016.1495.

Ramirez, R.M., and Craddock, R.A., 2018, The geological and climatological case for a warmer and wetter early Mars: Nature Geoscience, v. 11, p. 230–237, doi:10.1038/s41561-018-0093-9.

Reimer, P.J. et al., 2020, The IntCal20 Northern Hemisphere Radiocarbon Age Calibration Curve (0-55 cal kBP): Radiocarbon, v. 62, p. 725–757, doi:10.1017/RDC.2020.41.

Reneau, S.L., Dietrich, W.E., Dorn, R.I., Berger, C.R., and Rubin, M., 1986, Geomorphic and paleoclimatic implications of latest Pleistocene radiocarbon dates from colluvium-mantled hollows, California: Geology, v. 14, p. 655–658, doi:10.1130/0091-7613(1986)14<655:GAPIOL>2.0.CO;2.

Rhodes, E., 2011, Optically stimulated luminescence dating of sediments over the past 200,000 years: Annual Review of Earth and Planetary Sciences, v. 39, p. 461–488, doi:10.1146/annurev-earth-040610-133425.

Riding, R., 2000, Microbial carbonates the geological record of calcified bacterial–algal mats and biofilms: Sedimentology, v. 47, p. 179–214.

Rodríguez-Berriguete, Á., and Alonso-Zarza, A.M., 2019, Controlling factors and implications for travertine and tufa deposition in a volcanic setting: Sedimentary Geology, v. 381, p. 13–28, doi:10.1016/J.SEDGEO.2018.12.001.

Rossi, A.P., Neukum, G., Pondrelli, M., van Gasselt, S., Zegers, T., Hauber, E., Chicarro, A., and Foing, B., 2008, Large-scale spring deposits on Mars? Journal of Geophysical Research E: Planets, v. 113, p. 1–17, doi:10.1029/2007JE003062.

Rott, E., Holzinger, A., Gesierich, D., Kofler, W., and Sanders, D., 2010, Cell morphology, ultrastructure, and calcification pattern of Oocardium stratum, a peculiar lotic desmid: Protoplasma, v. 243, p. 39–50, doi:10.1007/s00709-009-0050-y.

Rypins, S., Reneau, S.L., Byrne, R., and Montgomery, D.R., 1989, Palynologic and geomorphic evidence for environmental change during the Pleistocene-Holocene transition at Point Reyes Peninsula, central coastal California: Quaternary Research, v. 32, p. 72–87, doi:10.1016/0033-5894(89)90033-1.

Saghaï, A. et al., 2015, Metagenome-based diversity analyses suggest a significant contribution of non-cyanobacterial lineages to carbonate precipitation in modern microbialites: Frontiers in Microbiology, v. 6, p. 1–16, doi:10.3389/fmicb.2015.00797.

Sancho, C. et al., 2015, Climatic implications of the Quaternary fluvial tufa record in the NE Iberian Peninsula over the last 500ka: Quaternary Research (United States), v. 84, p. 398–414, doi:10.1016/j.yqres.2015.08.003.

Sanders, D., and Rott, E., 2009, Contrasting styles of calcification by the micro-alga Oocardium stratum Naegeli 1849 (Zygnematophyceae) in two limestone-precipitating spring creeks of the Alps: Austrian Journal of Earth Sciences, v. 102, p. 34–49.

Sanders, D., Wertl, W., and Rott, E., 2010, Spring-associated limestones of the Eastern Alps: Overview of facies, deposystems, minerals, and biota: Facies, v. 57, p. 395–416, doi:10.1007/s10347-010-0252-y.

Schopf, J.W., 1993, Microfossils of the early Archean apex chert: New evidence of the antiquity of life: Science, v. 260, p. 640–646, doi:10.1126/science.260.5108.640.

Semikhatov, M.A., Gebelein, C.D., Cloud, P., Awramik, S.M., and Benmore, W.C., 1979, Stromatolite morphogenesis-progress and problems: Canadian Journal of Earth Sciences, v. 16, p. 992–1015.

Shiraishi, F., Okumura, T., Takahashi, Y., and Kano, A., 2010, Influence of microbial photosynthesis on tufa stromatolite formation and ambient water chemistry, SW Japan: Geochimica et Cosmochimica Acta, v. 74, p. 5289–5304, doi:10.1016/J.GCA.2010.06.025.

Shiraishi, F., Reimer, A., Bissett, A., de Beer, D., and Arp, G., 2008, Microbial effects on biofilm calcification, ambient water chemistry and stable isotope records in a highly supersaturated setting (Westerhöfer Bach, Germany): Palaeogeography, Palaeoclimatology, Palaeoecology, v. 262, p. 91–106, doi:10.1016/J.PALAEO.2008.02.011.

Spiro, B., and Pentecost, A., 1991, One day in the life of a stream—a diurnal inorganic carbon mass balance for a travertine-depositing stream (Waterfall Beck, Yorkshire): Geomicrobiology Journal, v. 9, p. 1–11, doi:10.1080/01490459109385981.

Stuiver, M., Reimer, P.J., and Reimer, R.W., 2021, CALIB 8.2 [WWW program] at http://calib.org, accessed 2021-5-10.

Suchý, V., Zachariáš, J., Tsai, H.C., Yu, T.L., Shen, C.C., Svetlik, I., Havelcová, M., Borecká, L., and Machovič, V., 2019, Relict Pleistocene calcareous tufa of the Chlupáčova sluj Cave, the Bohemian Karst, Czech Republic: A petrographic and geochemical record of hydrologically-driven cave evolution: Sedimentary Geology, v. 385, p. 110–125, doi:10.1016/j.sedgeo.2019.03.014.

Swart, P.K., 2015, The geochemistry of carbonate diagenesis: The past, present and future: Sedimentology, v. 62, p. 1233–1304, doi:10.1111/sed.12205.

Viles, H.A., and Pentecost, A., 2008, Tufa and Travertine: Geochemical Sediments and Landscapes, p. 173–199, doi:10.1002/9780470712917.ch6.

Viles, H.A., Taylor, M.P., Nicoll, K., and Neumann, S., 2007, Facies evidence of hydroclimatic regime shifts in tufa depositional sequences from the arid Naukluft Mountains, Namibia: Sedimentary Geology, v. 195, p. 39–53, doi:10.1016/j.sedgeo.2006.07.007.

Wagstaff, K.L., and Corsetti, F.A., 2010, An evaluation of information-theoretic methods for detecting structural microbial biosignatures: Astrobiology, v. 10, p. 363–379, doi:10.1089/ast.2008.0301.

Williford, K.H. et al., 2018, The NASA Mars 2020 Rover Mission and the Search for Extraterrestrial Life: Elsevier Inc., 275–308 p., doi:10.1016/b978-0-12-809935-3.00010-4.

Wordsworth, R.D., 2016, The Climate of Early Mars: Annual Review of Earth and Planetary Sciences, v. 44, p. 381–408, doi:10.1146/annurev-earth-060115-012355.

Appendix A: Distribution of ages for 'dark core' P1

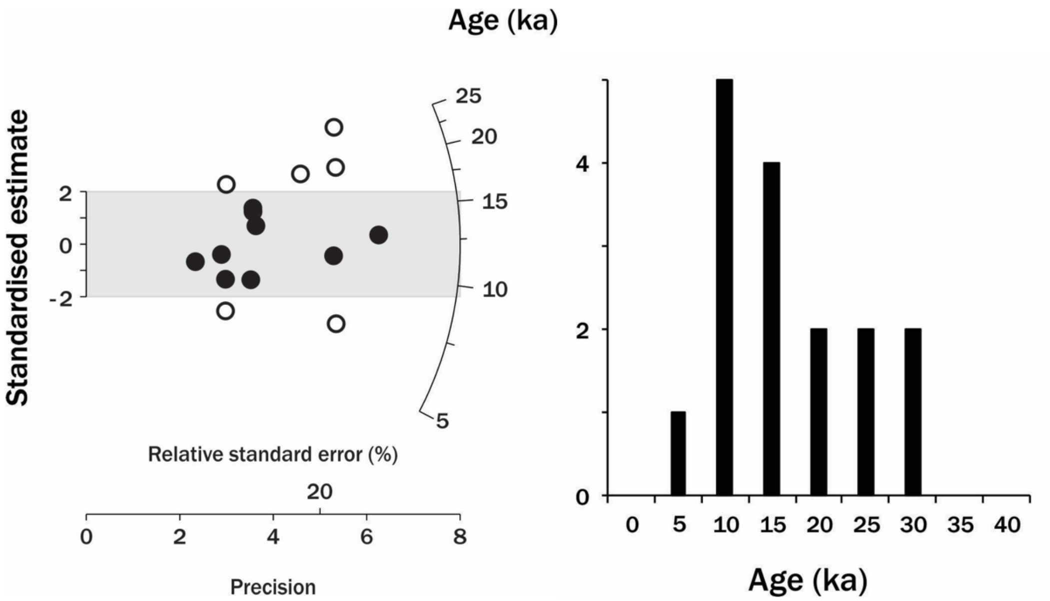

Appendix A. Age distributions, as a histogram and a radial plot, after fading correction (Huntley and Lamothe, 2001). Each circle on the radial plot represents the age and uncertainty, for a single aliquot. The age is read on the arc axis, by drawing a straight line from (0,0), passing through a circle and intersecting the radial axis (log scale). The (0,0) coordinate corresponds to a 0 standardized estimate (y-axis) and a 0 precision (x-axis), The uncertainty is read on the horizontal axis, by drawing a perpendicular line reaching a circle. Hence, two aliquots, having the same age, but with different uncertainty, will lay on the same straight line (from (0,0) to the radial axis). The aliquot with the smaller uncertainty (higher precision) will be closer to the arc. Values (filled circles) within the light grey shaded band are consistent (at 2s) with the weighted mean (Central Age Model). A cluster of aliquots within this shaded band express confidence that we have a population of grains consistent with a single age.